L Copy

TECHNICAL REPORT **3990**

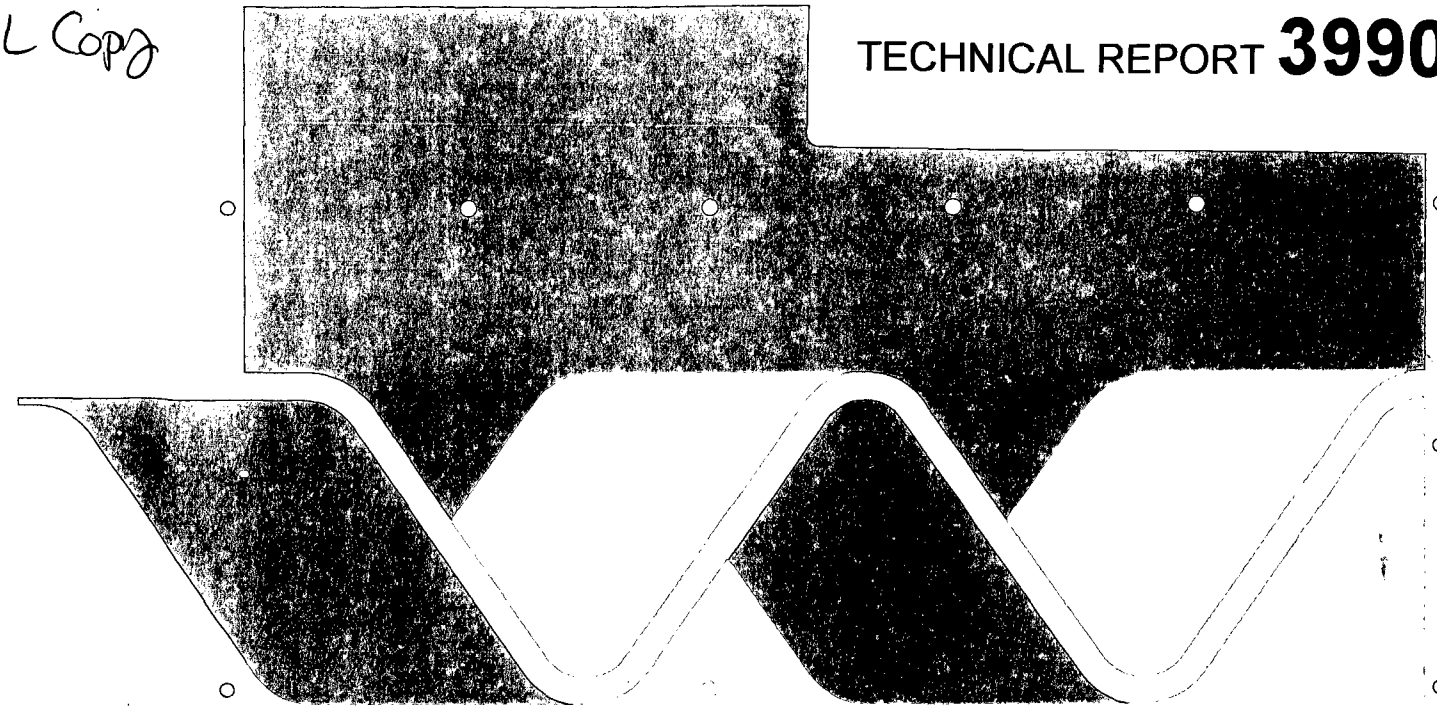

Manukau Harbour Dispersion Modelling

Part I

Preparation and verification of existing hydrodynamic model

Interim Report

March 1993

Z 472

delft hydraulics

Manukau Harbour Dispersion Modelling

Part I

Preparation and verification of existing hydrodynamic model

A.C. Bijlsma

delft hydraulics

delft hydraulics

CLIENT : Watercare Services Ltd., Auckland, New Zealand

TITLE : Manukau Harbour Dispersion Modelling
Preparation and verification of existing hydrodynamic model

ABSTRACT : A study is carried out on hydrodynamic and transport/dispersion computations for Manukau Harbour. The study is a continuation of the work of 1987 and 1989.
This Interim Report describes the preparation and conversion of the existing model for the improved hydrodynamic modelling system TRISULA, the preparation of field measurements and the verification of water levels and currents simulated by the model for a Mean Neap Tide (18 April 1974), and a Mean Spring Tide (2 December 1970). Drogue releases of 17 and 20 April 1991 were also used for verification.
From the results of the verification it was concluded that the present version of the hydrodynamic model of Manukau Harbour reproduces the results of the previous version satisfactory. Accordingly, the quality of dispersion studies will be similar to those based on the previous model version. This quality is sufficient for an overall scanning of the impact of various outfall locations, as was the case in previous studies.

REFERENCES: DELFT HYDRAULICS, Proposal dated 16 September 1992 (FAX518.92/z472.95/aw)
Watercare Services, Letter of commission dated 19 October 1992 (File 10/10/31/10)

REV.	ORIGINATOR	DATE	REMARKS	CHECKED BY	APPROVED BY
0	A.C. Bijlsma	26 March 1993			A. Roelfzema

KEYWORD(S)	NO. OF PAGES	DOCUMENT NO.	STATUS
	TEXT : 7 TABLES : 4 FIGURES : 21	VR449.93	☐ PRELIMINARY ☐ DRAFT ■ FINAL
	FILE CODE: z472t02.wp0		

Contents

List of tables

List of figures

List of appendices

1 Introduction

In 1987 DELFT HYDRAULICS performed a mathematical model study to predict the effects of discharges of treated effluent on the water quality of Manukau Harbour near Auckland, New Zealand. The study served to support the Auckland Regional Authority in their decisions on the disposal of effluent. This study was performed in association with Beca Carter Hollings and Ferner Ltd., principal consultant to the Auckland Regional Authority. The results were reported in (DELFT HYDRAULICS, 1987). To simulate the worst conditions in view of water quality, the mathematical model tests were performed for Neap Tide conditions only. Further to the study of 1987, Beca Carter Hollings and Ferner Ltd. commissioned DELFT HYDRAULICS in 1988 to perform additional mathematical model computations which include a Spring Tide condition, see (DELFT HYDRAULICS, 1989).

In 1992, Watercare Services Ltd. required further hydrodynamic and transport/dispersion computations for Manukau Harbour. In view of the developments since 1988 in modelling software and hardware infrastructure, the availability of new measurement datasets and the possible need for more accurate simulations in this stage of the Manukau Harbour project, Watercare services commissioned Option 3 of DELFT HYDRAULICS' Proposal of 16 September 1992 (FAX518.92/Z472.95/aw). This Interim Report relates to Task 1 ("Preparation"), Task 2 ("Preparation of field measurements and verification runs") and Task 3 ("Reporting"). On the basis of these results it would be decided whether the execution of Task 4 ("refinement and recalibration") is necessary.

2 Preparation and conversion of model definition files

From the archives of the 1987 and 1988 work on Manukau Harbour hydrodynamic and dispersion modelling, see (DELFT HYDRAULICS, 1987 and 1989), the relevant input and data files on model schematisation and model simulations have been retrieved. This information was converted into a set of files that defines the Manukau Harbour Model (depth-averaged flow) in our improved hydrodynamic modelling system TRISULA. A detailed description of TRISULA is given in Appendix A. Figures 2.1 and 2.2 give the layout of the model and the schematisation of the curvilinear grid, respectively. The location of various water level and current Stations is presented in Fig. 2.3.

Two characteristic tidal conditions are available for simulation:

A) Mean Neap Tide (on 18 April 1974) from (DELFT HYDRAULICS, 1987), and
B) Mean Spring Tide (2 December 1970) from (DELFT HYDRAULICS, 1989).

The simulations are cyclic with a period of 12.5 hours.

3 Preparation of field measurements

New field measurements have been carried out by the New Zealand Oceanographic institute (NZOI) at two locations.

i) In Papakura Channel moored current meter observations were gathered by NZOI from 4-26 April 1991, while drogue observations were carried out on 17, 20, 22 and 28 April. Relevant parts of the Data and Analysis Report have been made available, see (NZOI, 1991). Information on the drogue observations of 22 and 28 April (including a Neap Tide period) were not provided to DELFT HYDRAULICS.
   This Report includes the most important tidal constants of the water levels at Onehunga. Combined with the Admiralty Tide Tables (Hydrographer of the Navy, 1988) a set of 7 constituents (O_1, K_1, N_2, M_2, S_2, M_4, MS_4) is available for water level predictions at Onehunga, see Table 3.1.
   Sets of tidal constants are given for the currents (in alongshore direction) at the Upper and the Lower current meter. The Upper meter (instrument height 18 m, water depth 26 m) can be used for comparison with the depth-averaged flow as computed by the model. Its tidal constants are given in Table 3.2.

ii) In Purakau Channel current meter observations were performed by NZOI from 28 September to 20 October 1992. A floppy disk with the data and documentation has been provided to DELFT HYDRAULICS. Information on current speed and direction was transformed into time-series for east and north velocity components which were then subject to tidal analysis. The resulting sets of tidal constants (see Tables 3.3 and 3.4) permit the prediction of the local tidal currents. Given the instrument height of 7 m and the water depth of 15 m, these prediction can be directly compared with (depth-averaged) model results.

The tidal analysis were carried out, using DELFT HYDRAULICS' programme package GETIJSYS. Tidal predictions and the determination of times of high water in view of the verification below, will be done with the same package.

4 Verification runs

For the verification of the Manukau Harbour Model, runs for the conditions A and B above (Mean Neap Tide and Mean Spring Tide, resp.) have been performed. The results will be evaluated for water levels, currents and drogue tracks. Since a relatively large spring tide occurs on 15-16 April 1991, data related to the drogue tests on 17 and 20 April 1991 have been compared with results of the Mean Spring computation.

4.1 Water levels

Fig. 4.1 presents the computed and predicted water levels at Onehunga for three periods: those of conditions A and B, and those of 20 April 1991 as well. The times of high water at Onehunga have been used to align the model results with the local time frame used for measurements and predictions.
The comparison of water levels at Onehunga (predicted by O_1, K_1, M_2 and S_2, like in the previous studies) is good and resembles that of Fig. 6.6 from (DELFT HYDRAULICS, 1987).

4.2 Currents

The results of the velocity verification (condition A) of the previous model are given in Figs. 6.9 - 6.12 of (DELFT HYDRAULICS, 1987). They represent the currents in the main inlet to the harbour (Fig. 6.9), the first division in separate channels (Fig. 6.10), Papakura Channel (Fig. 6.11) and the northern Channel (Fig. 6.12). Results of the present model version are shown in Figs. 4.2-4.5 attached to this report (in the same order). The results compare generally well, even in a number of characteristic details. An exception must be made for the magnitude of the extreme currents at station 4, though.
The results of the velocity verification (condition B) of the previous model are given in Figs. 2.2 - 2.5 of (DELFT HYDRAULICS, 1989). Results of the present model version are shown in Figs. 4.6-4.9 (in the same order). Again, the results compare well, including some characteristic details. In this computation Station 4 compares well. It was not possible to recover the reason for the above anomaly, however.
From the above comparison it can be concluded that the present model version has the same performance compared to the previous model version.

The feasibility of the model at the two new measurement locations is illustrated by the following two figures.
Fig. 4.10 shows for conditions A and B that at the new measurement location in Papakura Channel the model gives a reasonable estimate of the current in alongshore direction. This is in agreement with the earlier verifications in this Channel.
Fig. 4.11 presents the result at the new measurement location in Purakau Channel. Here, the maximum currents are somewhat underestimated by the present model. Of course the model performance can be improved by further calibration or grid refinement.

4.3 Drogue tests

A further indication of the feasibility of the model for further studies can be given by simulation of the drogue tests of (NZOI, 1991). The drogue releases of 17 and 20 April in Papakura Channel were simulated with model in a Mean Spring Tide Computation. The resulting drogue tracks are presented in Figs. 4.12-4.18. The drogues are released at the bar, at a distance of two grid cells. The time of release is given at the bottom of the figure. The position of the drogues is marked every 15 minutes after release. The general comparison with corresponding figures of the measurements in (NZOI, 1991) is satisfactory, given the detail of the model and its boundary conditions. The largest difference, occurring for the drogues of Fig. 4.17, is due to a mismatch in release location.

5 Conclusions

Summarizing, we conclude that the present version of the Manukau Harbour Model reproduces the results of the previous version satisfactory. Therefore, the quality of the hydrodynamic results (tidal water levels and currents) and the dispersion will be similar to those based on the previous model version.
This quality is sufficient for an overall scanning of the impact of various outfall locations, as was the case in the previous studies.

References

DELFT HYDRAULICS, 1987. Auckland Area Sewerage Study, Manukau Harbour Dispersion Modelling. Prepared for Auckland Regional Authority. Report Z226, October 1987.

DELFT HYDRAULICS, 1989. Auckland Area Sewerage Study, Manukau Harbour Dispersion Modelling (Additional Computations). Prepared for Auckland Regional Authority. Report Z292, January 1989.

Hydrographer of the Navy, 1988. Admiralty Tide Tables and Tidal Stream Tables, Volume 3, 1989. NP 203-89.

NZOI, 1991. New Zealand Oceanographic Institute. Current measurements and drogue tests in Papakura Channel (April 1991). Pp. 8-17, Figs., Tables. Addendum to letter 10/10/31/10 of ARC Water Services, 20 August 1992.

Table 3.1 Tidal constants of the water level at Onehunga.
(Amplitudes in m, phases in degrees, local time, zone -12:00 h.)

```
+ DELFT HYDRAULICS
+ P.O. BOX 177 2600 MH  DELFT
+ PROJECT CODE : Z-472, DATE: 09-12-1992
+ TIDAL prediction Onehunga
+ PERIOD: 17 Apr 1991 00:00 - 17 Apr 1991 24:00
910417  000000
910418  000000
m
         7
O1        0.02        111.0
K1        0.06        207.0
N2        0.27        284.0
M2        1.35        301.0
S2        0.36        355.0
M4        0.06         43.0
MS4       0.03        104.0
   15,
    1
910417  000000   2.37       .00000
```

Table 3.2 Tidal constants of the along shore current component, Papakura Channel.
(Amplitudes in m/s, phases in degrees, local time)

```
+ DELFT HYDRAULICS
+ P.O. BOX 177 2600 MH  DELFT
+ PROJECT CODE : Z-472, DATE: 11-12-1992
+ TIDAL prediction Papakura, currents in along-shore direction (90 deg)
+ Water depth: 26 m, Meter height: 18 m (upper current meter)
+ PERIOD of interest:  2 Dec 1970
701115  000000
701215  000000
m
         5
N2        0.139       240.0
M2        0.812       228.0
S2        0.203       262.0
M4        0.068       325.0
MS4       0.036        27.0
   15,
    1
701115  000000   0.00       .00000
```

Table 3.3 Tidal constants of the east current component, Purakau Channel. (Amplitudes in m/s, phases in degrees, local time)

```
+ DELFT HYDRAULICS
+ P.O. BOX 177 2600 MH  DELFT
+ PROJECT CODE : Z-472, DATE: 09-12-1992
+ TIDAL ANALYSIS u-velocity measurement from Purakau Channel
+ PERIOD: 28 Sep 1992 13:50 - 20 Oct 1992 12:10
+ U-velocity from speed/dir file cm92arc1.dat
+ cm92arc1.dat                20-OCT-92  MJG      filename  processing code
+ s4 05451240                                     instrument id. & tape number
+ 36 58.64S   174 42.49E                          lat long
+ Purakau Channel, Manukau Harbour.               description of location
+   15      7                                     water depth,meter height -m
+ 1350 28  9 92   1210 20 10 92   12              record start/finish time & zone
+    0  0 10  0                                   data gap interval d,h,m,s
+ S4 on for   1 mins  every  10 mins. Ave count: 120.   SRB count:   6
+ The time given in the data is the start of each 'on time' period.
+ ARC contract deployment.

 BLOCK FOR INSTRUMENTS

  INSTRUMENT    1 : TIMESTEP     =    .166667
  INSTRUMENT    1 : MEAN LEVEL   =    .051232
  INSTRUMENT    1 : LINEAR TREND =   -.000079


 BLOCK FOR SUBSERIES

   PERIOD  1       TO =  6781.00       YEAR     = 1992
 START TIME    =  6517.83 HOURS AFTER 1 JAN
 END   TIME    =  7044.17 HOURS AFTER 1 JAN

 NUMBER OF COMPONENTS   :    41

 NAME      AMPLITUDE   PHASE (G)        FREQUENCY (OM)   VO + U      F

 MSO           .028      317.6          1.015895816      307.5     1.004
 O1            .011        1.4         13.943035702      306.2     1.007
 K1            .014       68.8         15.041068623      132.3     1.004
 P1            .005       68.8         14.958930564      266.6     1.000
 2KO1          .004      351.9         16.139102499      318.4     1.015
 3MS2          .003      217.1         26.952311740      187.6     1.011
 MNS2          .010      202.1         27.423833104      291.2     1.007
 MU2           .035      266.2         27.968207556      133.0     1.004
 N2            .105      199.5         28.439730828      238.6     1.004
 NU2           .020      199.5         28.512582007      336.9     1.004
 2N2           .014      199.5         27.895354469       34.7     1.004
 M2            .510      210.6         28.984103372       82.5     1.004
 LABDA2        .000      210.6         29.455624736        8.2     1.004
 S2            .133      255.3         29.999999188       30.0     1.000
 K2            .038      255.3         30.082137247       84.6      .989
 MSN2          .031      163.8         30.544373639      233.9     1.007
 2SM2          .018       83.7         31.015895004      337.5     1.004
 2MK3          .002       95.1         42.927138120       32.8     1.012
 MK3           .006       61.9         44.025171995      214.8     1.008
 SK3           .007       33.7         45.041067811      162.3     1.004
 3MS4          .016      293.7         56.952310927      217.6     1.011
 MN4           .030      171.0         57.423834199      321.2     1.007
 M4            .043      203.7         57.968206743      165.1     1.007
 SN4           .008      359.7         58.439730015      268.6     1.004
 MS4           .019      212.2         58.984102559      112.5     1.004
 2MSN4         .006      111.4         59.528478918      316.5     1.011
 S4            .010      269.9         59.999998375       60.0     1.000
 3MK5          .002      191.6         71.911245306      115.3     1.015
 3MO5          .005       59.7         73.009275367      301.4     1.017
 4MS6          .001       51.1         85.936414299      300.2     1.014
 2MN6          .006      239.6         86.407933756       43.7     1.011
 M6            .020      305.9         86.952313930      247.6     1.011
 MSN6          .008      307.0         87.423833387      351.2     1.007
 2MS6          .021      317.5         87.968205931      195.1     1.007
 3MSN6         .001      184.3         88.512586104       39.0     1.014
 2SM6          .001       80.0         88.984105562      142.5     1.004
 3MN8          .014      183.6        115.392040943      126.2     1.014
 M8            .021      273.9        115.936413487      330.2     1.014
 2MSN8         .005      275.6        116.407932944       73.7     1.011
 3MS8          .028      292.3        116.952313117      277.6     1.011
 2(MS)8        .003      254.1        117.968205119      225.1     1.007

 STANDARD DEVIATION    :      .0477
```

Table 3.4 Tidal constants of the north current component, Purakau Channel. (Amplitudes in m/s, phases in degrees, local time)

```
+ DELFT HYDRAULICS
+ P.O. BOX 177 2600 MH  DELFT
+ PROJECT CODE : Z-472, DATE: 09-12-1992
+ TIDAL ANALYSIS v-velocity measurement from Purakau Channel
+ PERIOD: 28 Sep 1992 13:50 - 20 Oct 1992 12:10
+ V-velocity from speed/dir file cm92arc1.dat
+ cm92arc1.dat                  20-OCT-92  MJG      filename  processing code
+ s4 05451240                                      instrument id. & tape number
+ 36 58.64S   174 42.49E                           lat long
+ Purakau Channel, Manukau Harbour.                description of location
+   15      7                                       water depth,meter height - m
+ 1350 28  9 92   1210 20 10 92   12               record start/finish time & zone
+   0  0 10  0                                     data gap interval d,h,m,s
+ S4 on for   1 mins  every  10 mins. Ave count: 120.   SRB count:   6
+ The time given in the data is the start of each 'on time' period.
+ ARC contract deployment.

 BLOCK FOR INSTRUMENTS

  INSTRUMENT    1 : TIMESTEP     =    .166667
  INSTRUMENT    1 : MEAN LEVEL   =    .019480
  INSTRUMENT    1 : LINEAR TREND =   -.000058

 BLOCK FOR SUBSERIES

   PERIOD  1      TO =  6781.00      YEAR     = 1992
 START TIME    =  6517.83 HOURS AFTER 1 JAN
 END   TIME    =  7044.17 HOURS AFTER 1 JAN

 NUMBER OF COMPONENTS   :    41

 NAME     AMPLITUDE   PHASE (G)        FREQUENCY (OM)   VO + U     F

 MS0          .019      300.4          1.015895816      307.5    1.004
 O1           .013      358.4         13.943035702      306.2    1.007
 K1           .010       68.3         15.041068623      132.3    1.004
 P1           .003       68.3         14.958930564      266.6    1.000
 2KO1         .005      354.1         16.139102499      318.4    1.015
 3MS2         .006      214.9         26.952311740      187.6    1.011
 MNS2         .009      216.1         27.423833104      291.2    1.007
 MU2          .020      267.6         27.968207556      133.0    1.004
 N2           .062      193.2         28.439730828      238.6    1.004
 NU2          .012      193.2         28.512582007      336.9    1.004
 2N2          .008      193.2         27.895354469       34.7    1.004
 M2           .298      208.0         28.984103372       82.5    1.004
 LABDA2       .000      208.0         29.455624736        8.2    1.004
 S2           .068      251.6         29.999999188       30.0    1.000
 K2           .019      251.6         30.082137247       84.6     .989
 MSN2         .017      160.9         30.544373639      233.9    1.007
 2SM2         .013       72.4         31.015895004      337.5    1.004
 2MK3         .004       64.0         42.927138120       32.8    1.012
 MK3          .008       23.7         44.025171995      214.8    1.008
 SK3          .003       34.6         45.041067811      162.3    1.004
 3MS4         .011      312.7         56.952310927      217.6    1.011
 MN4          .017      181.7         57.423834199      321.2    1.007
 M4           .026      239.8         57.968206743      165.1    1.007
 SN4          .006       63.8         58.439730015      268.6    1.004
 MS4          .003      213.2         58.984102559      112.5    1.004
 2MSN4        .007      135.2         59.528478918      316.5    1.011
 S4           .003      232.6         59.999998375       60.0    1.000
 3MK5         .003      246.2         71.911245306      115.3    1.015
 3MO5         .005       40.9         73.009275367      301.4    1.017
 4MS6         .002      289.4         85.936414299      300.2    1.014
 2MN6         .011      185.7         86.407933756       43.7    1.011
 M6           .018      257.5         86.952313930      247.6    1.011
 MSN6         .003      105.9         87.423833387      351.2    1.007
 2MS6         .012      280.9         87.968205931      195.1    1.007
 3MSN6        .005      102.1         88.512586104       39.0    1.014
 2SM6         .001      198.3         88.984105562      142.5    1.004
 3MN8         .006      158.0        115.392040943      126.2    1.014
 M8           .007      255.1        115.936413487      330.2    1.014
 2MSN8        .002      274.6        116.407932944       73.7    1.011
 3MS8         .013      271.3        116.952313117      277.6    1.011
 2(MS)8       .002      259.8        117.968205119      225.1    1.007

 STANDARD DEVIATION     :      .0363
```

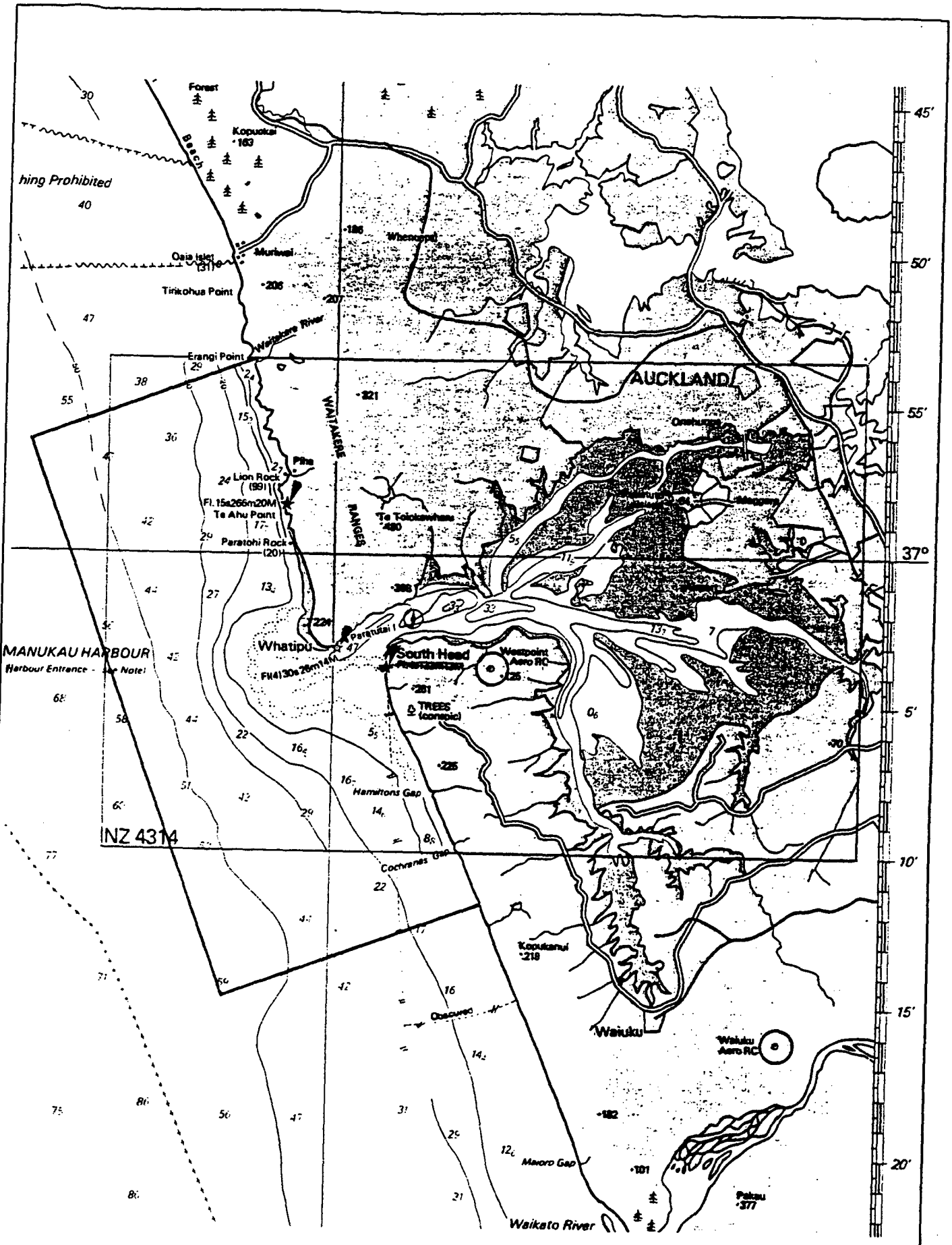

Layout and bathymetry of the hydrodynamic model of Manukau Harbour	21-12-92	
	TRISULA	
Delft Hydraulics	z-472-20	Fig. 2.1

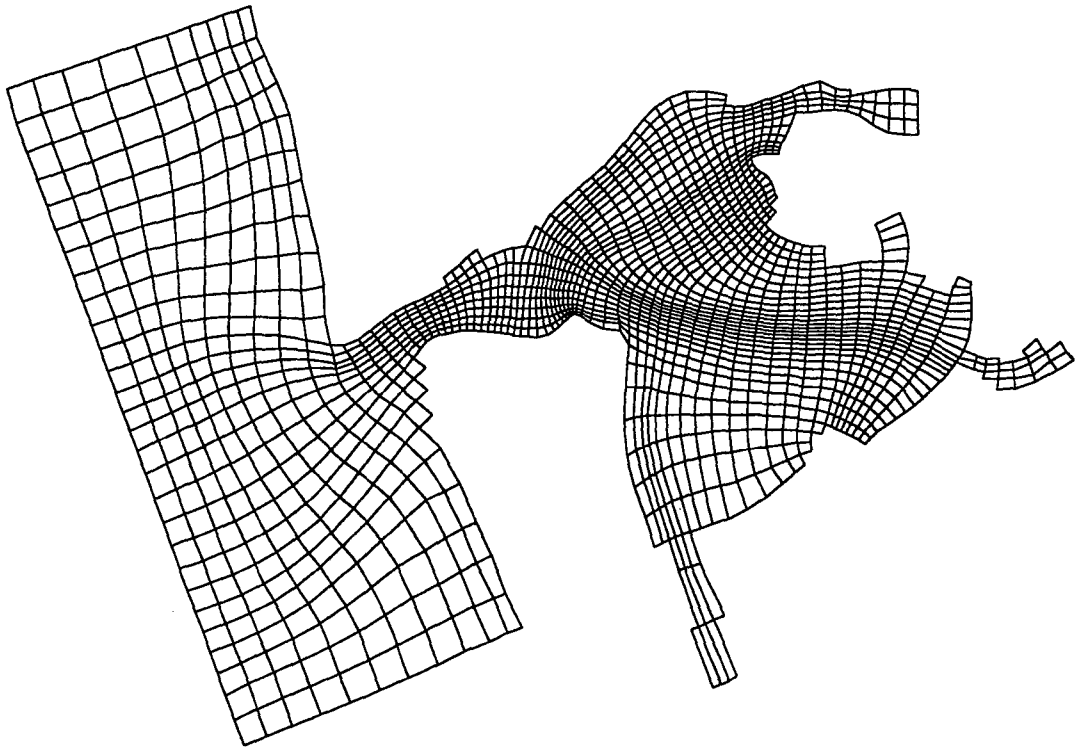

Curvilinear grid of the
Manukau Harbour model

21-12-92

TRISULA

Delft Hydraulics

z-472-20

Fig. 2.2

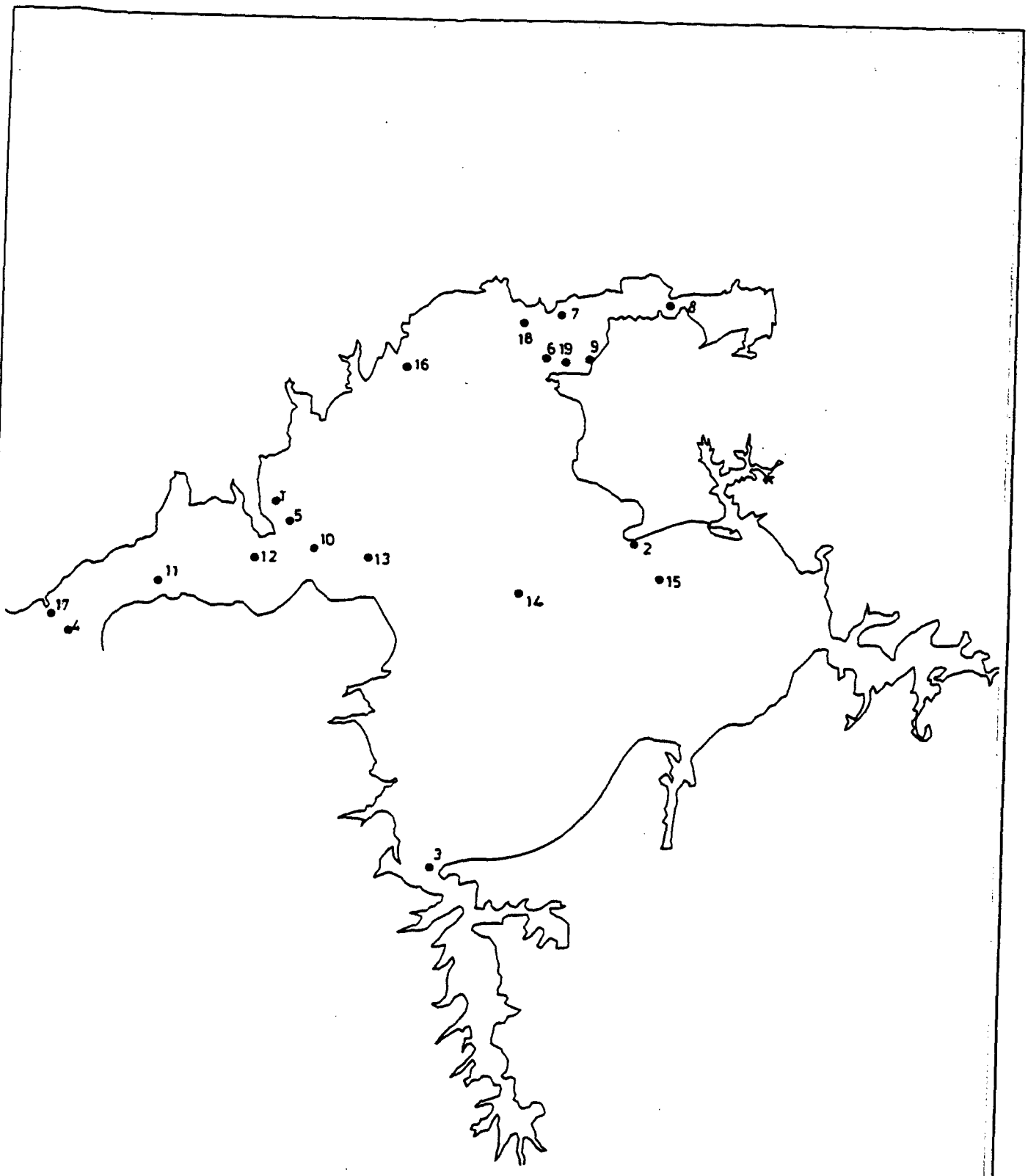

Location of water level and current stations	21-12-92	
	TRISULA	
Delft Hydraulics	z-472-20	Fig. 2.3

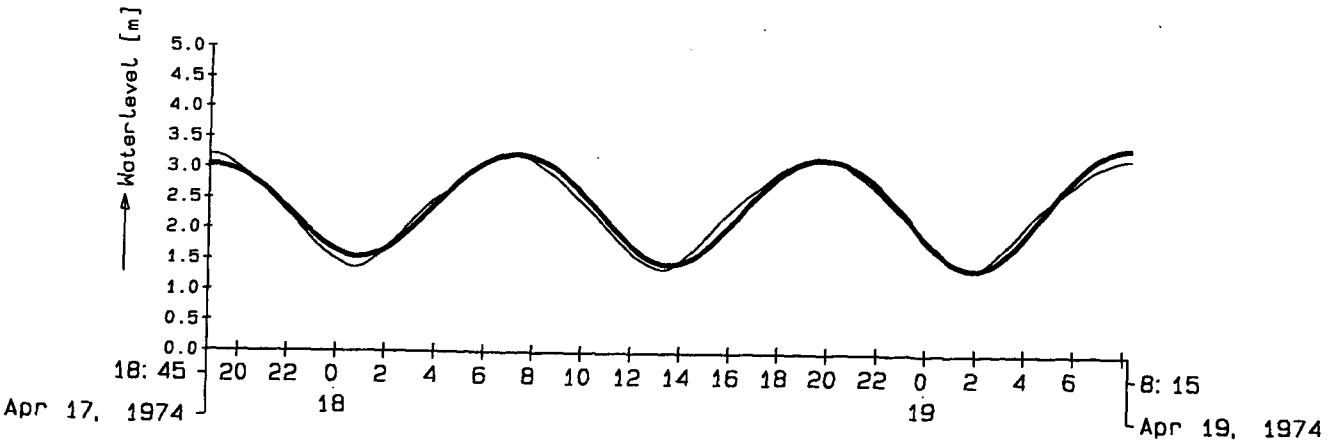

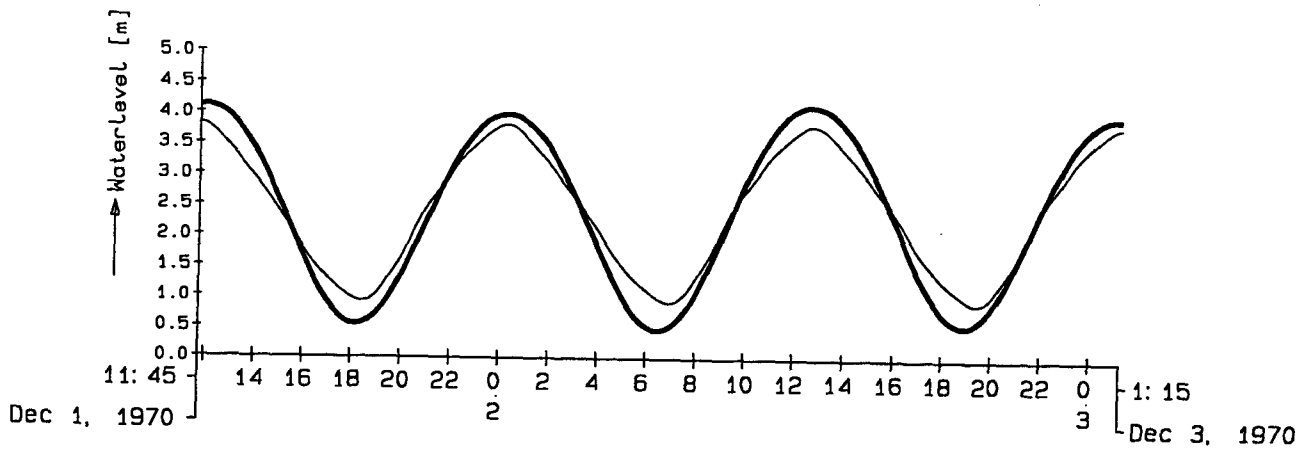

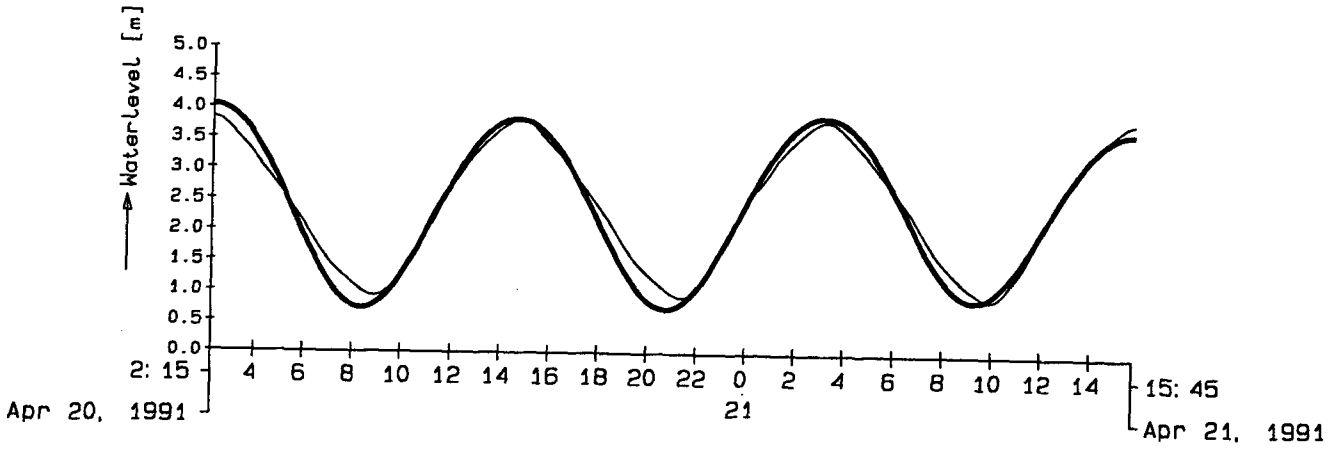

Predicted
Computed

Waterlevel Onehunga (c/nz4315) Chart Datum
Mean neap tide (1974/04/18) and
mean spring tides (1970/12/02 and 1991/04/20)

21-12-92	033/043
TRISULA	
z-472-20	Fig. 4.1

Delft Hydraulics

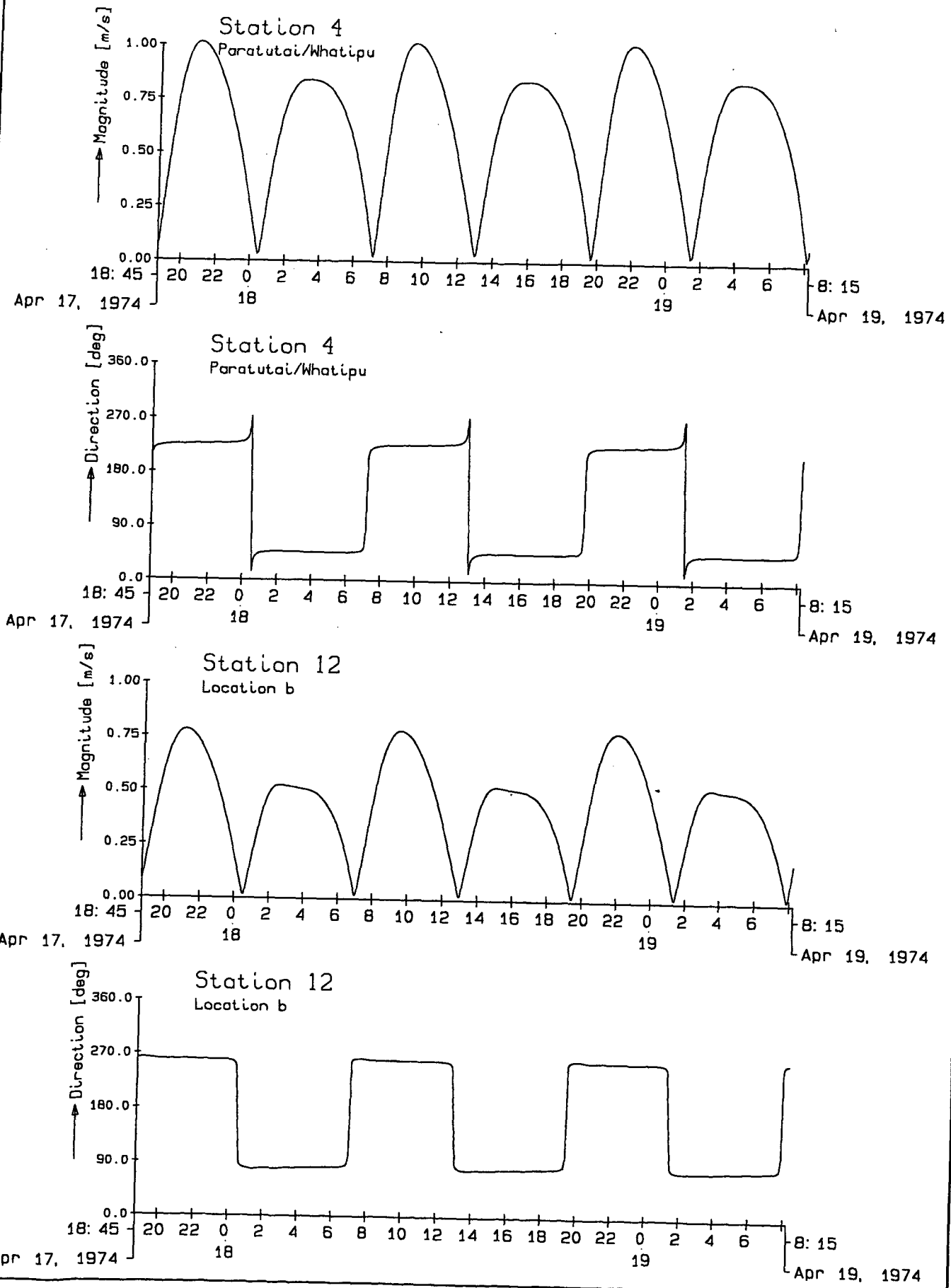

Mean neap tide (1974/04/18)
Magnitude and direction of velocity, station 4 and 12

21-12-92	033
TRISULA	
z-472-20	Fig. 4.2

Delft Hydraulics

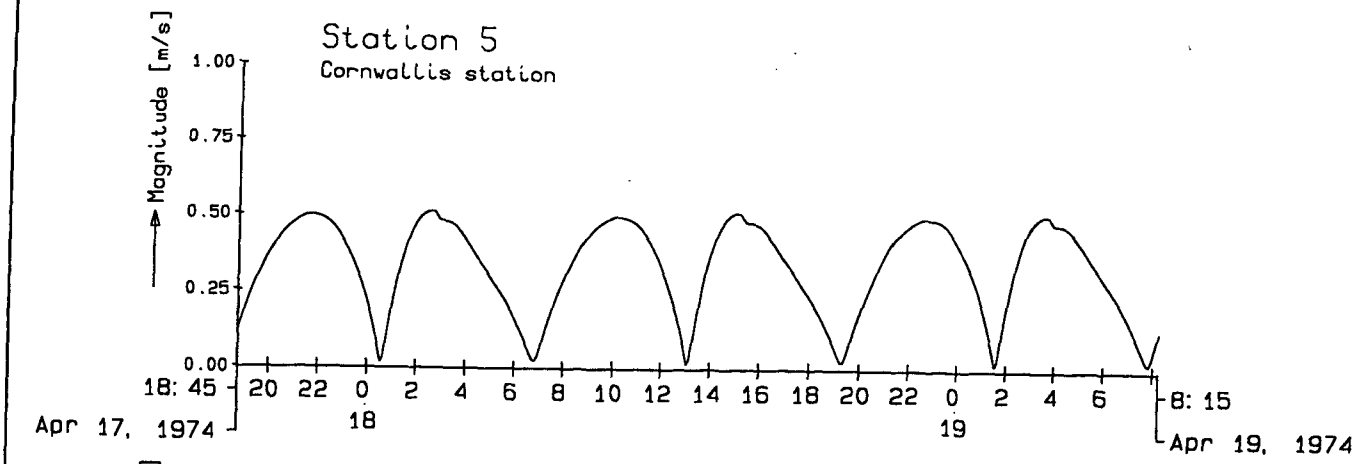

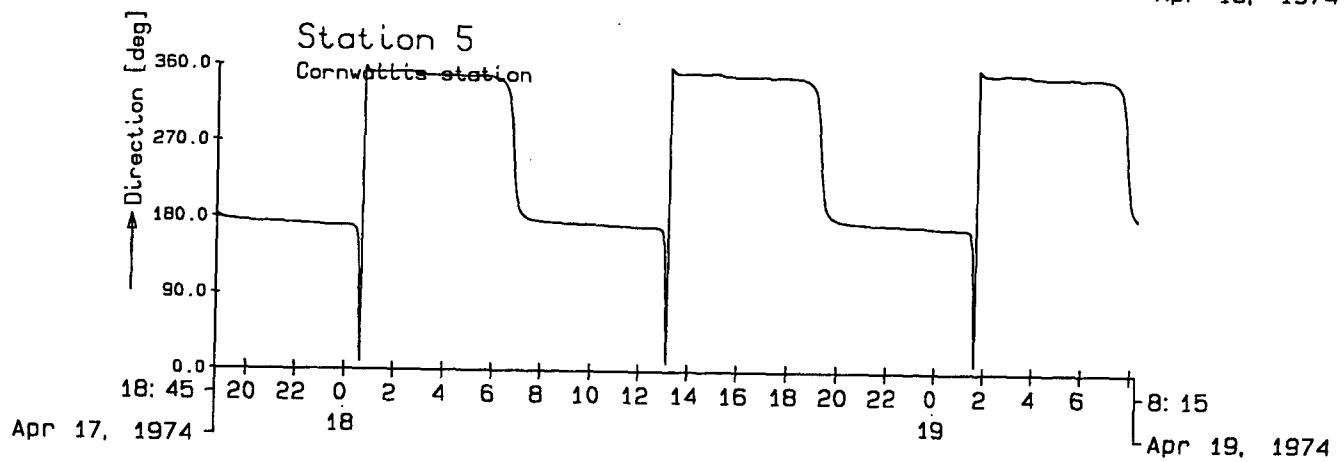

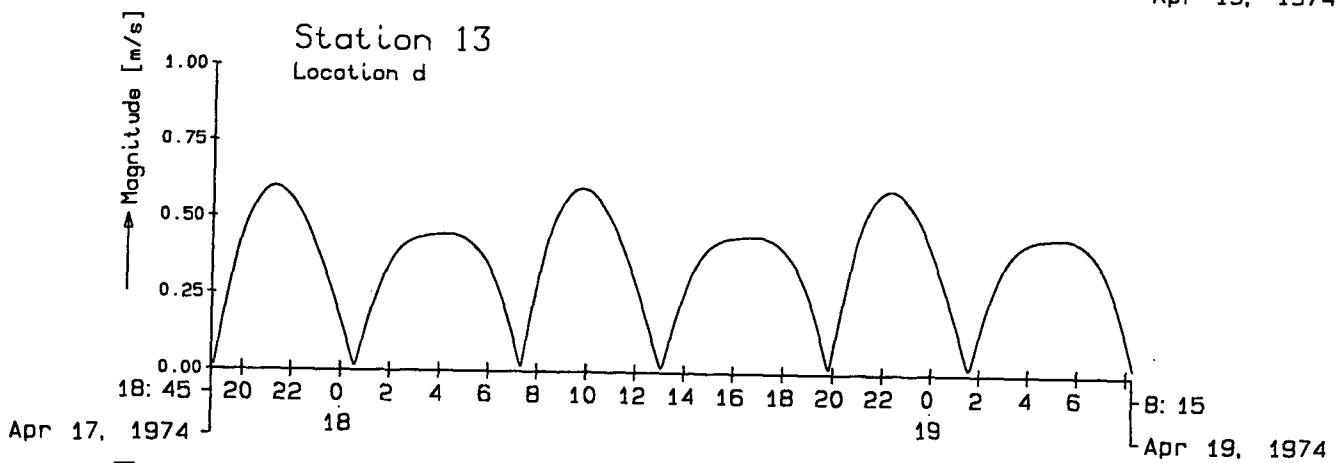

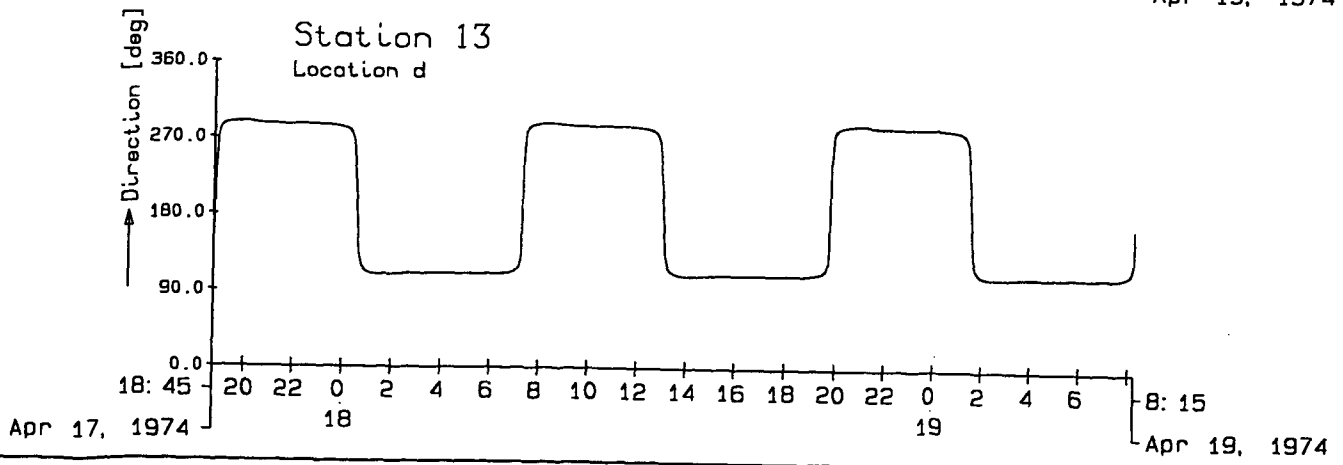

Mean neap tide (1974/04/18)
Magnitude and direction of velocity, station 5 and 13

21-12-92	033
TRISULA	
z-472-20	Fig. 4.3

Delft Hydraulics

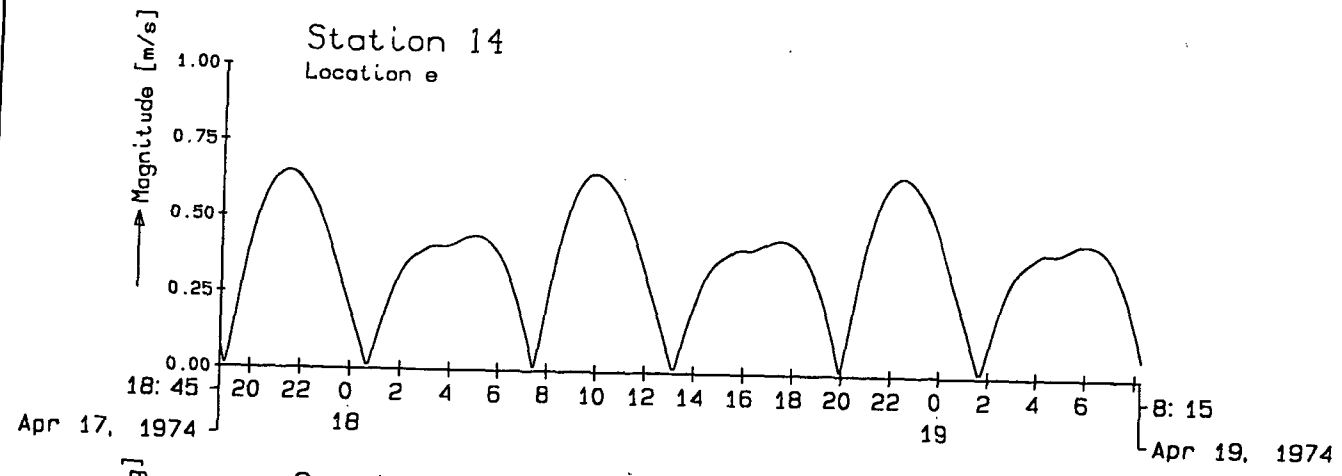

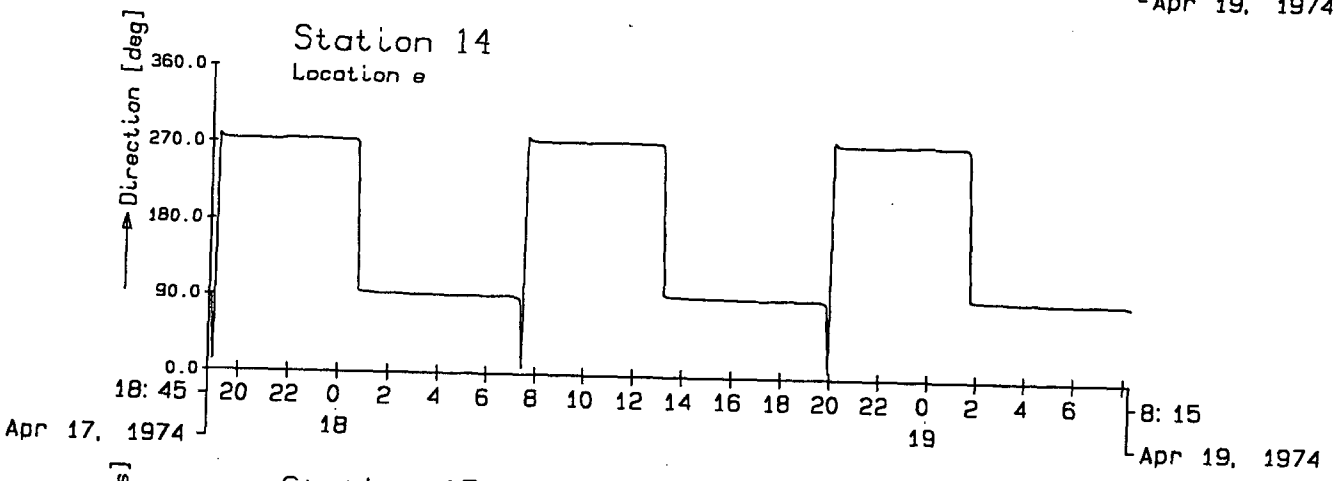

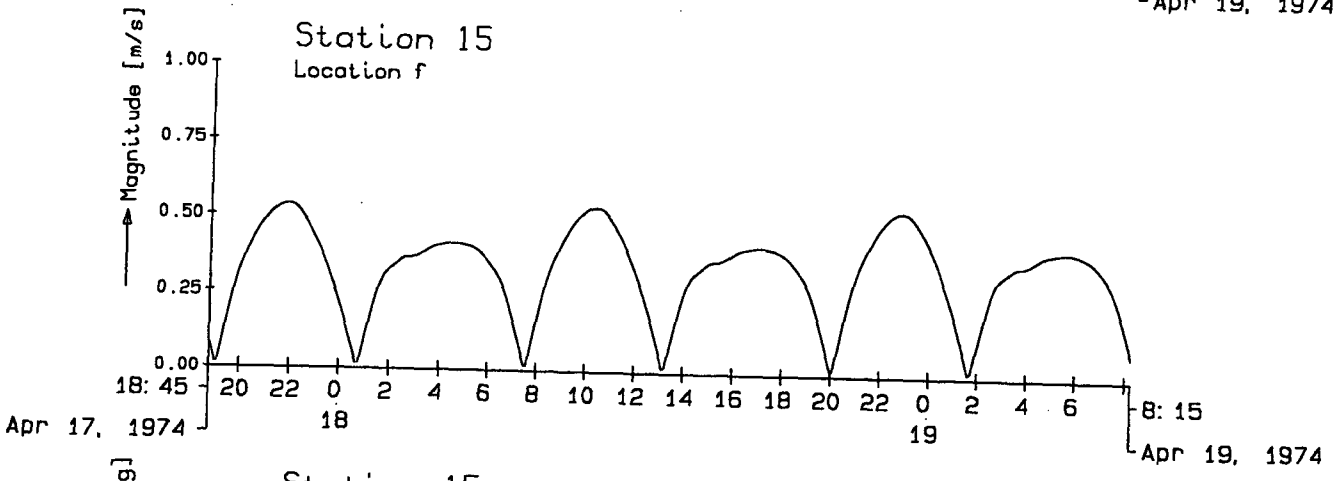

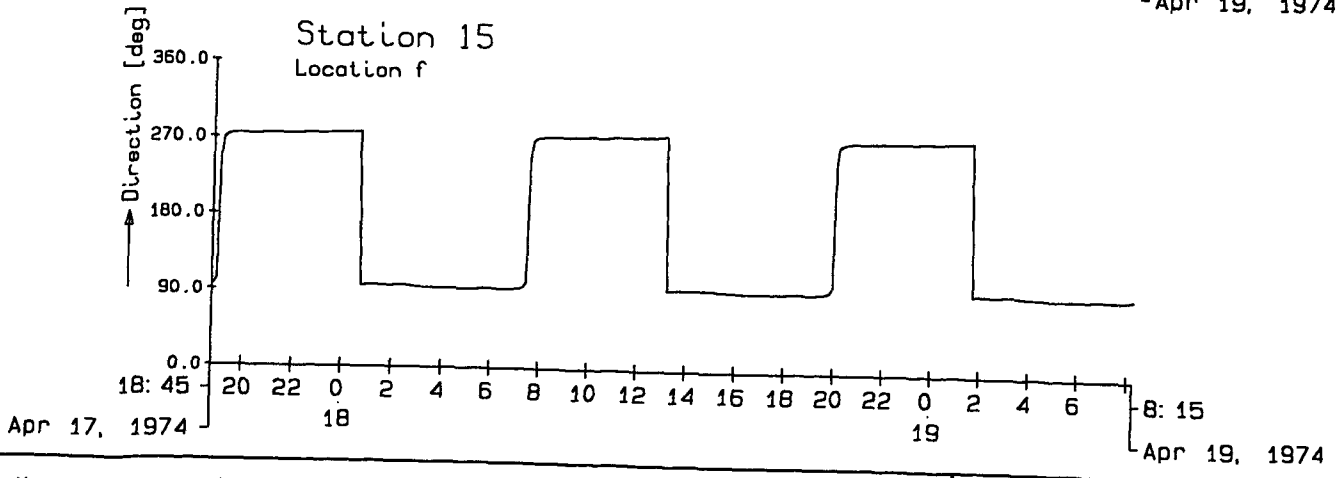

Mean neap tide (1974/04/18)
Magnitude and direction of velocity, station 14 and 15

21-12-92	033
TRISULA	
z-472-20	Fig. 4.4

Delft Hydraulics

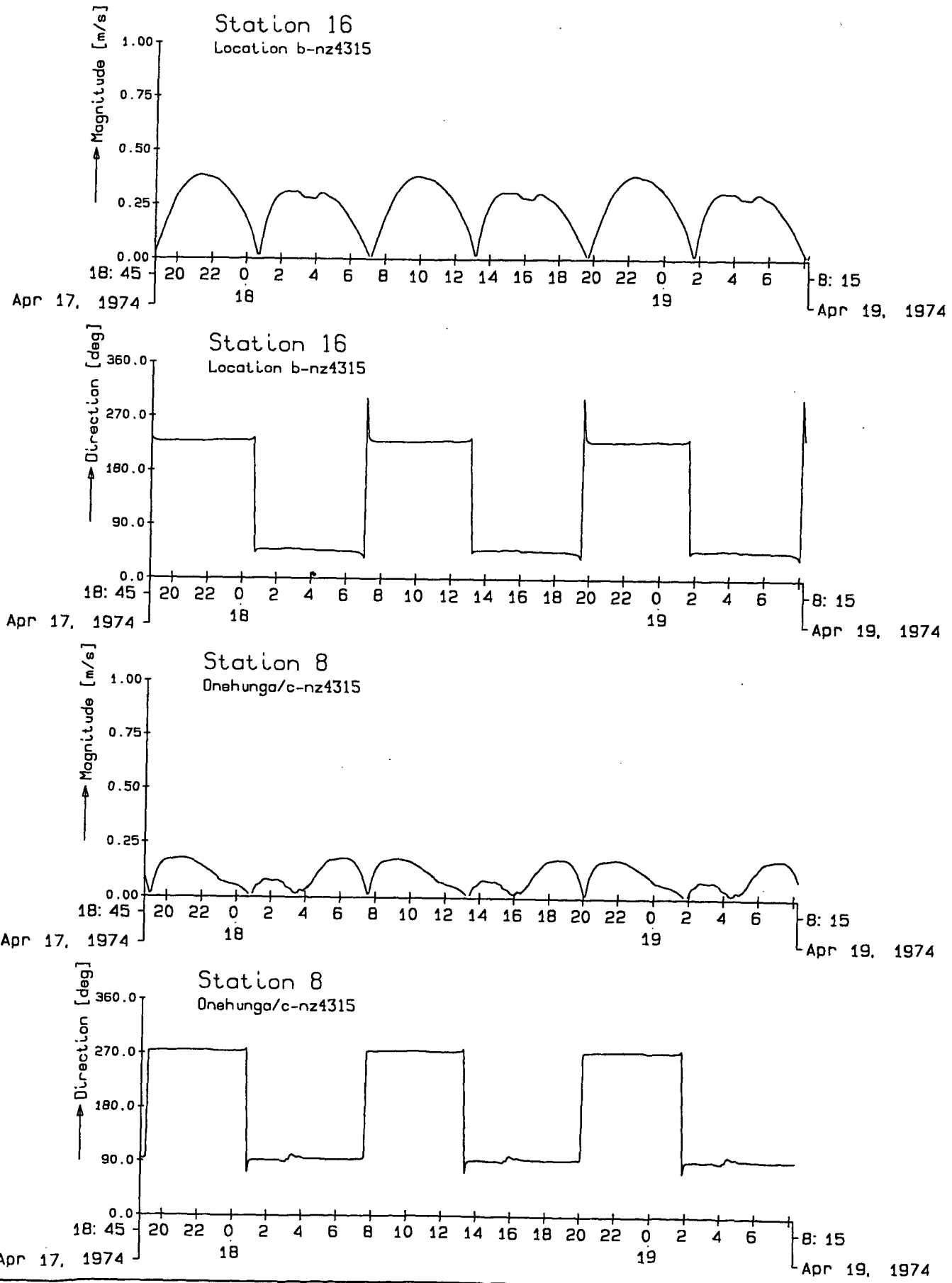

Mean neap tide (1974/04/18)
Magnitude and direction of velocity, station 16 and 8

21-12-92	033
TRISULA	
z-472-20	Fig. 4.5

Delft Hydraulics

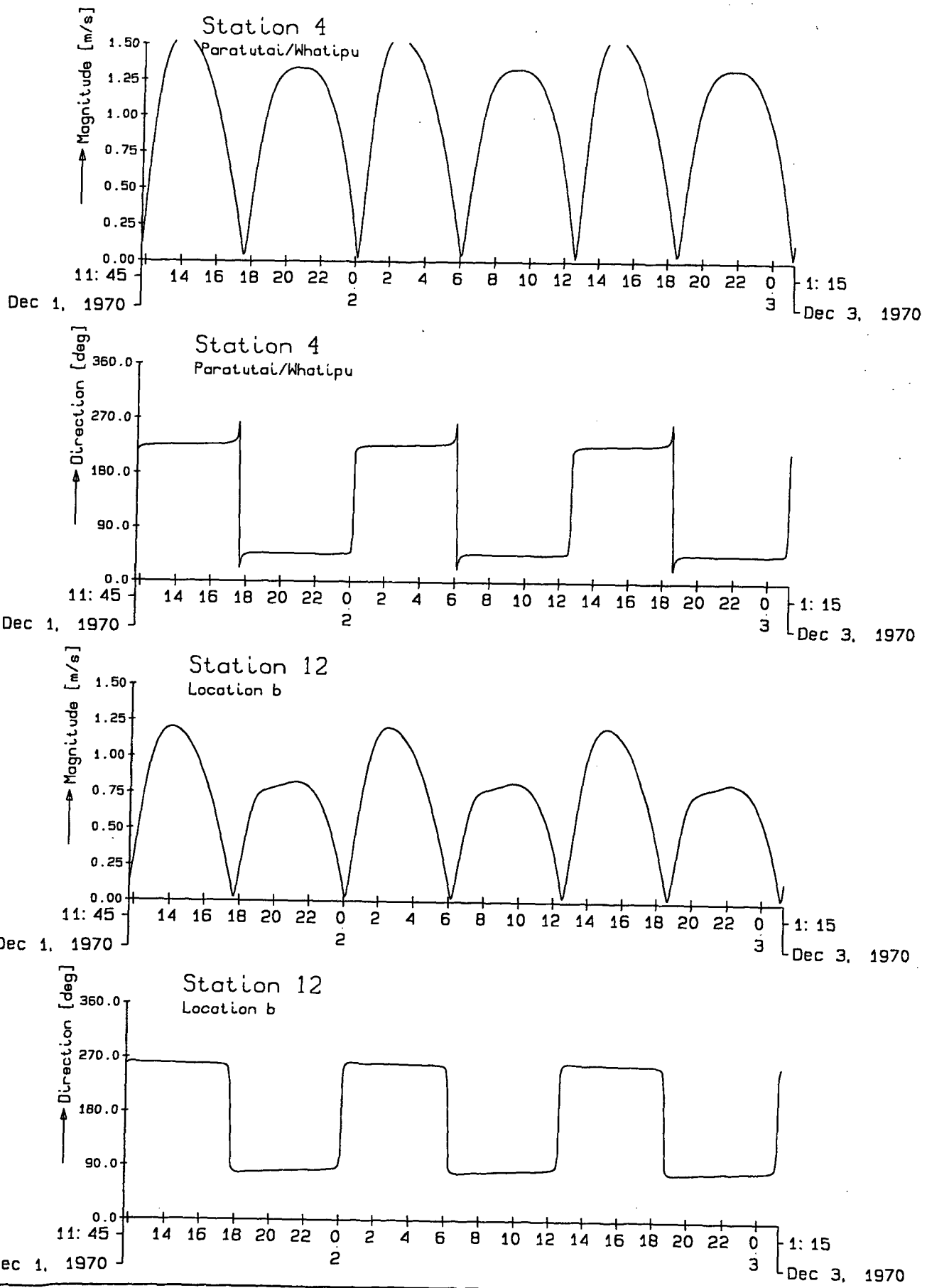

Mean spring tide (1970/12/02)
Magnitude and direction of velocity, station 4 and 12

21-12-92	043
TRISULA	
z-472-20	Fig. 4.6

Delft Hydraulics

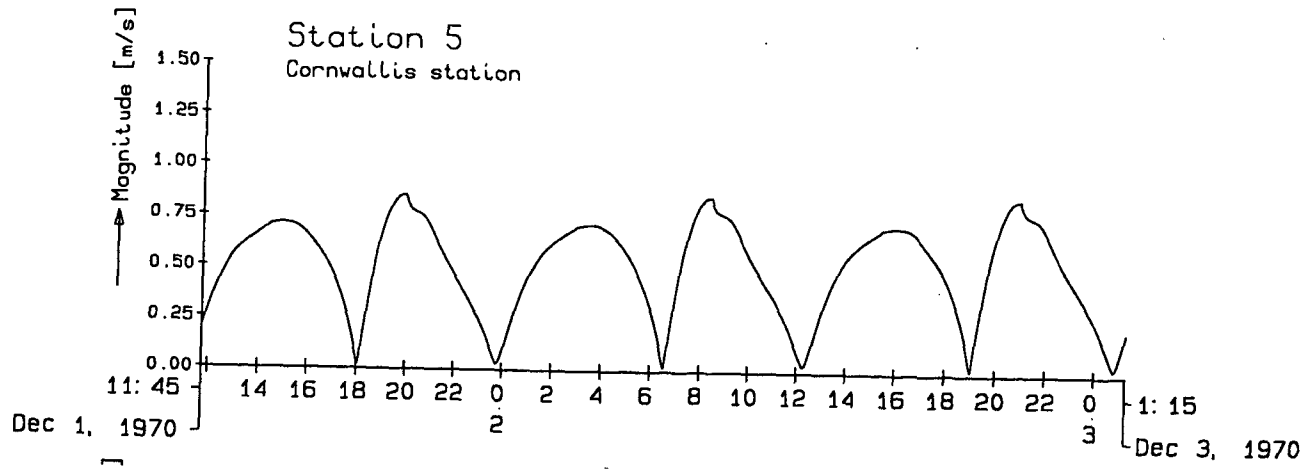

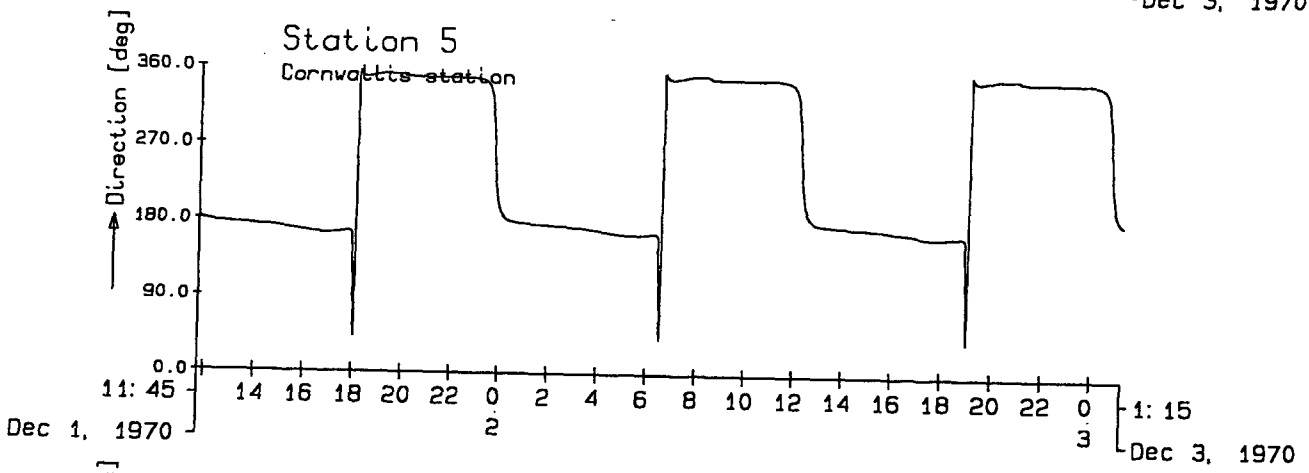

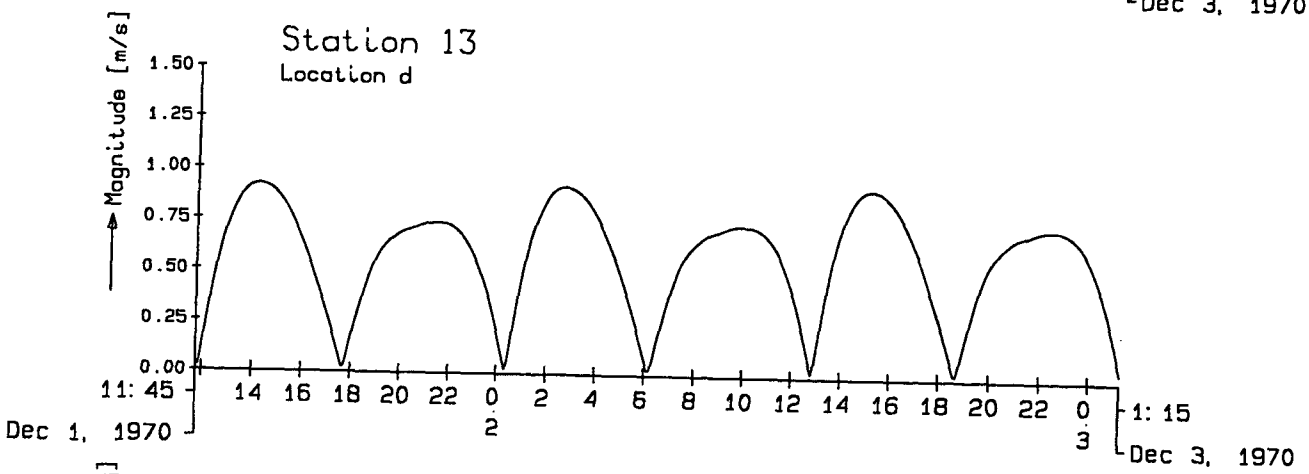

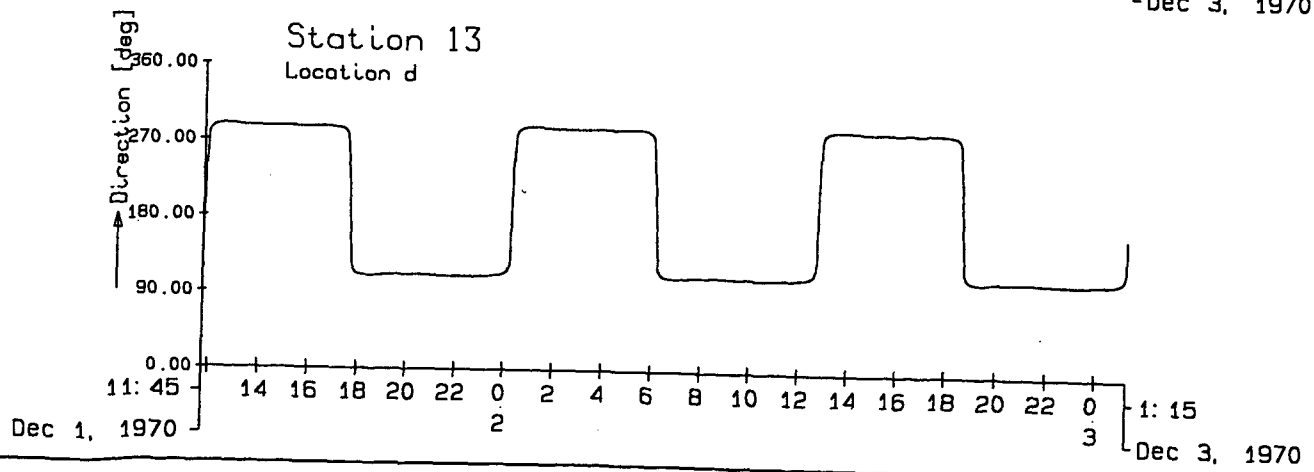

Mean spring tide (1970/12/02)
Magnitude and direction of velocity, station 5 and 13

21-12-92	043
TRISULA	
z-472-20	Fig. 4.7

Delft Hydraulics

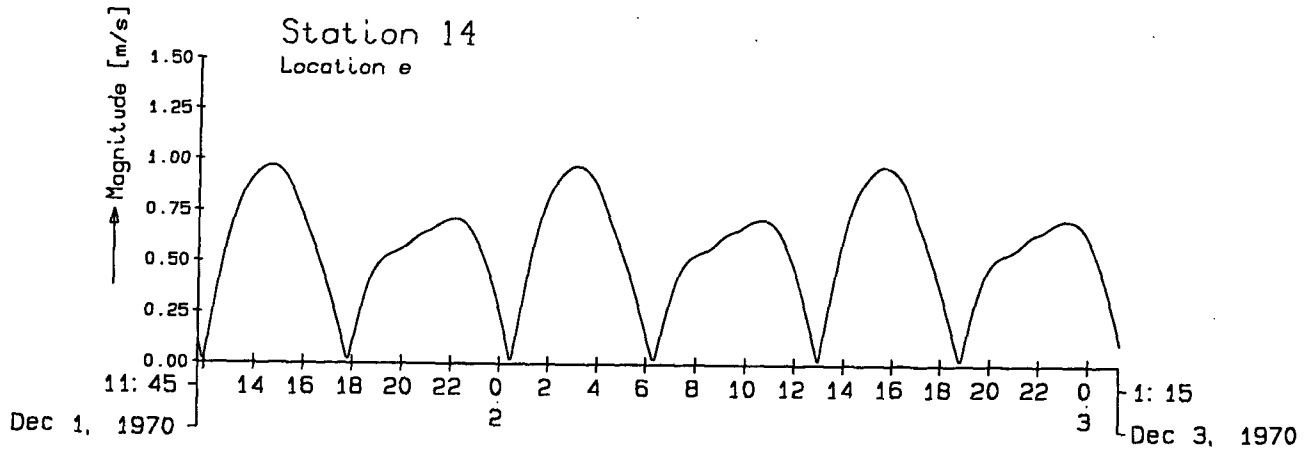

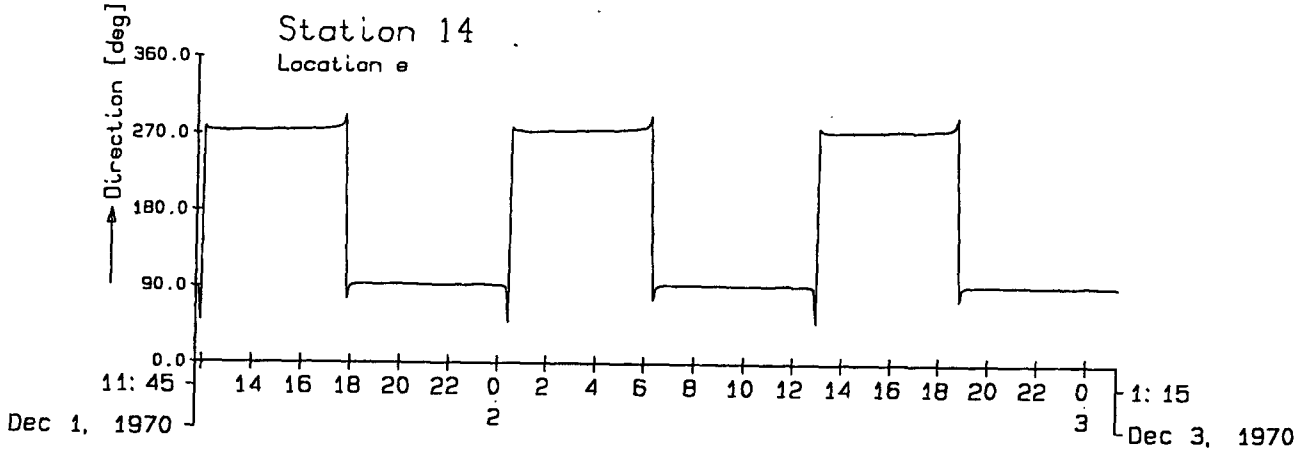

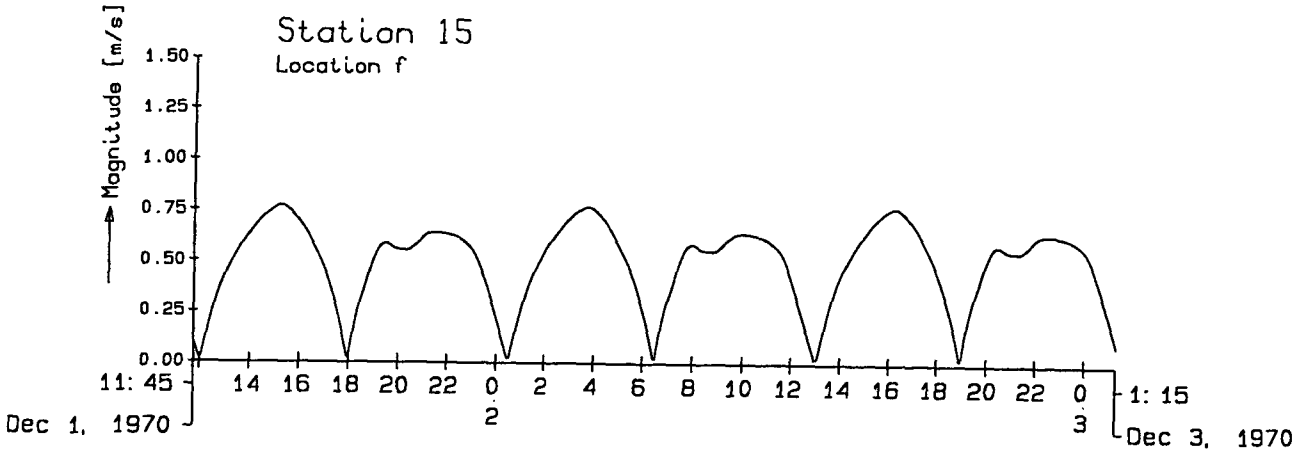

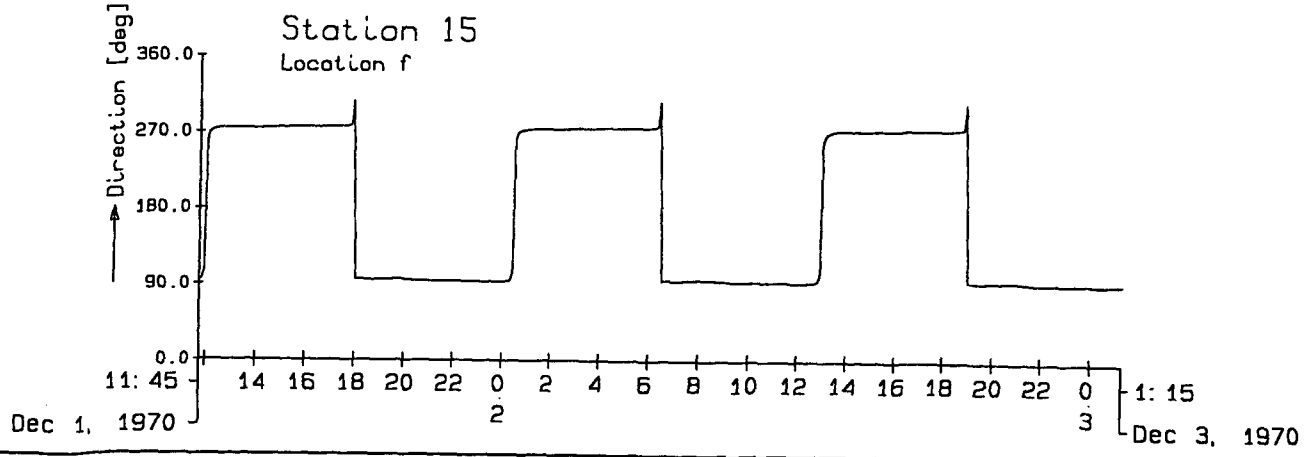

Mean spring tide (1970/12/02)
Magnitude and direction of velocity, station 14 and 15

21-12-92	043
TRISULA	
z-472-20	Fig. 4.8

Delft Hydraulics

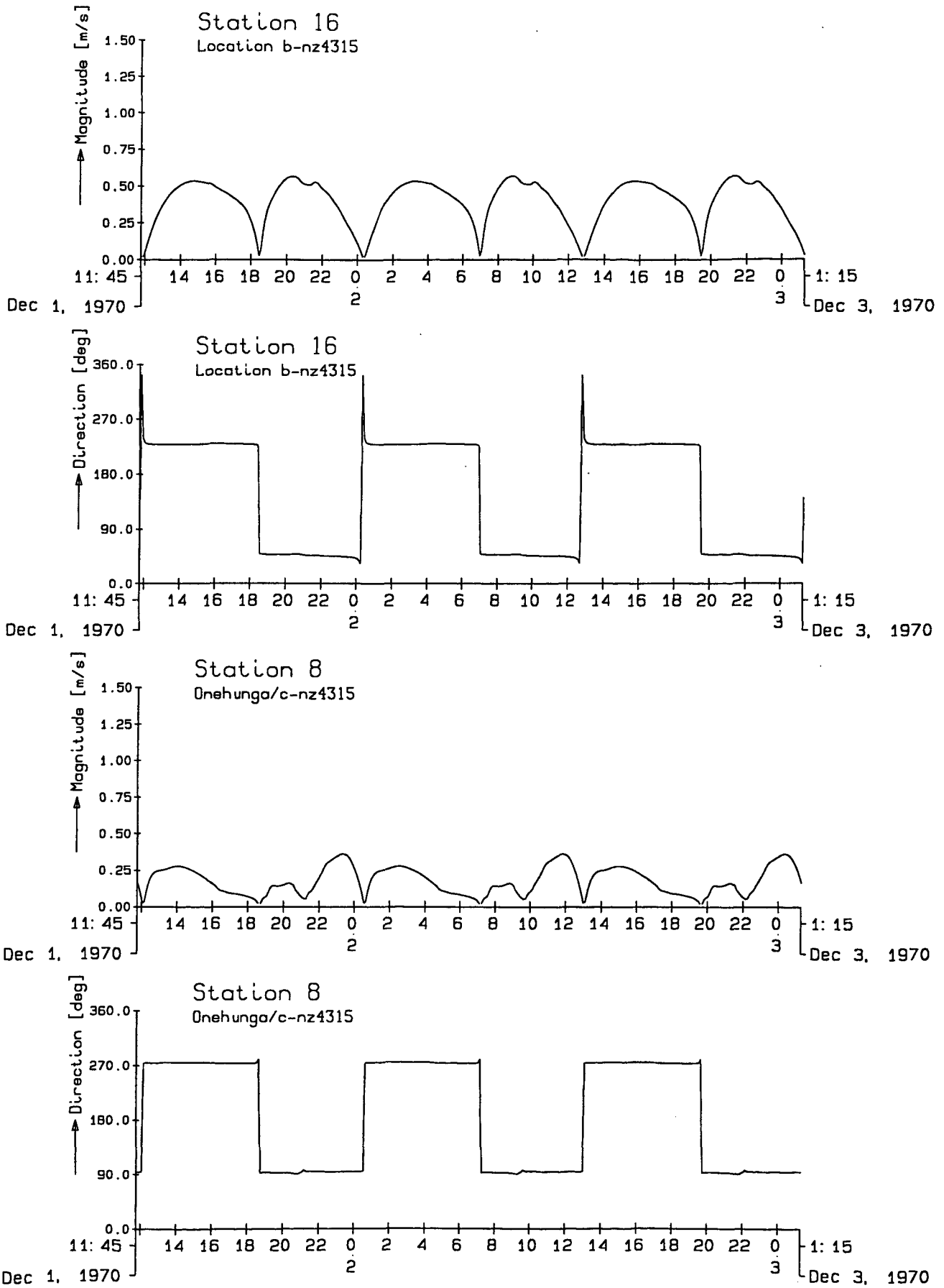

Mean spring tide (1970/12/02)
Magnitude and direction of velocity, station 16 and 8

21-12-92	043
TRISULA	
Delft Hydraulics	z-472-20 Fig. 4.9

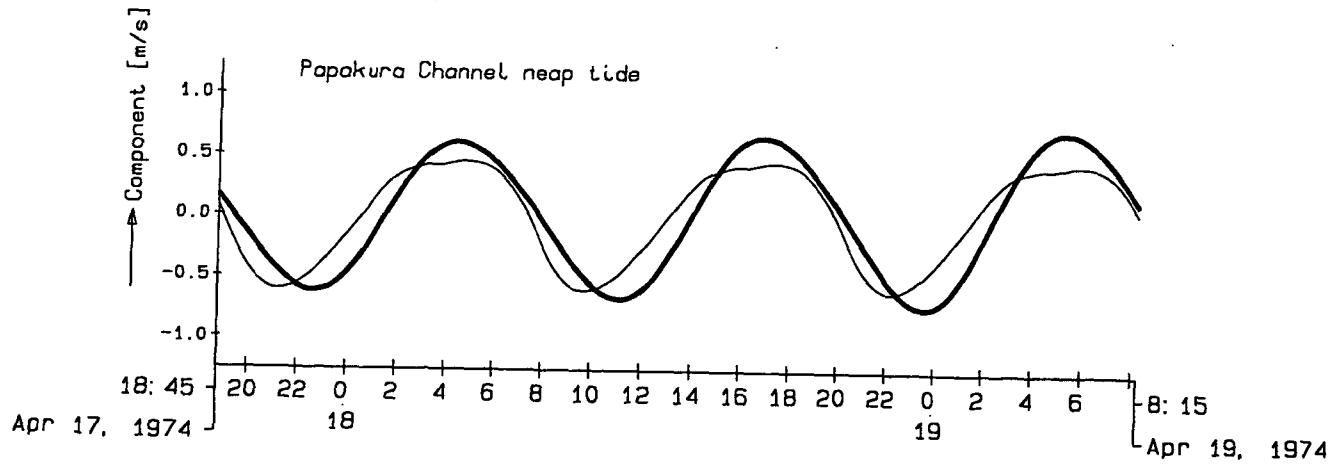

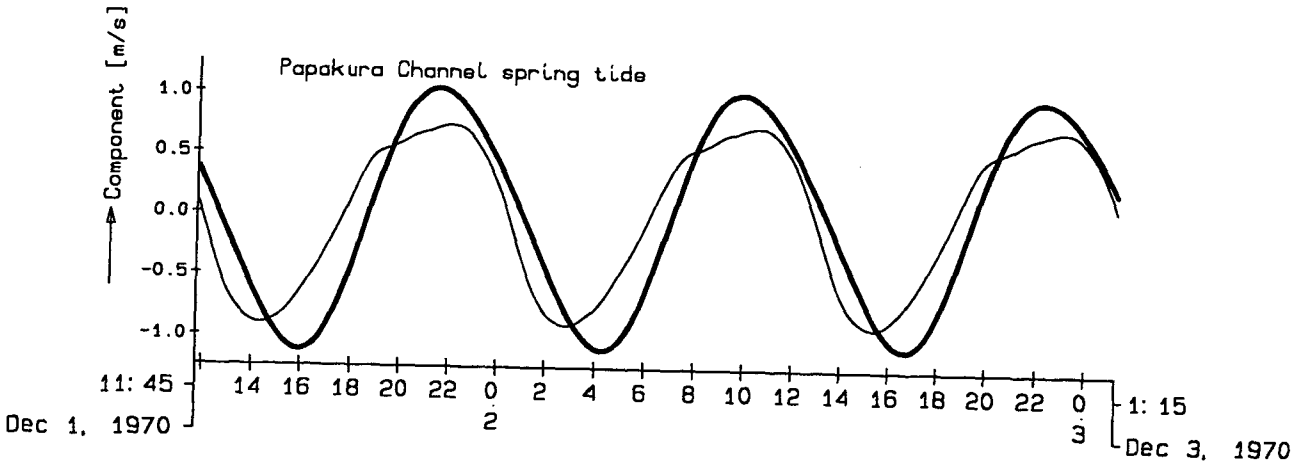

Predicted
Computed

Mean neap [1974/04/18] and
mean spring tide [1970/12/02]
Alongshore velocity component Papakura channel

21-12-92	033/043
TRISULA	
z-472-20	Fig. 4.10

Delft Hydraulics

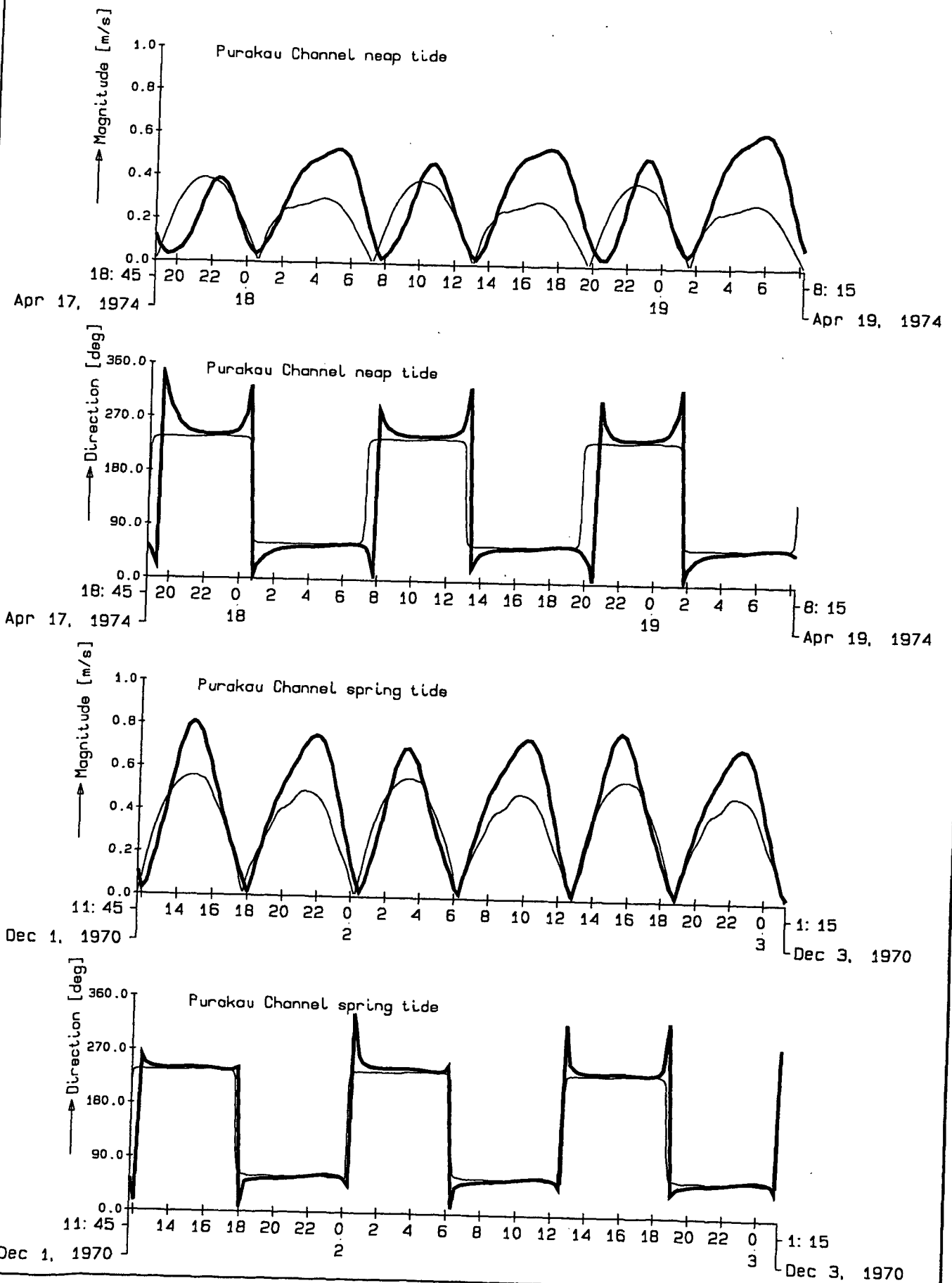

Predicted ——— Computed

Mean neap (1974/04/18) and
mean spring tide (1970/12/02)
Magnitude and direction of velocity Purakau channel

21-12-92	033/043
TRISULA	
z-472-20	Fig. 4.11

Delft Hydraulics

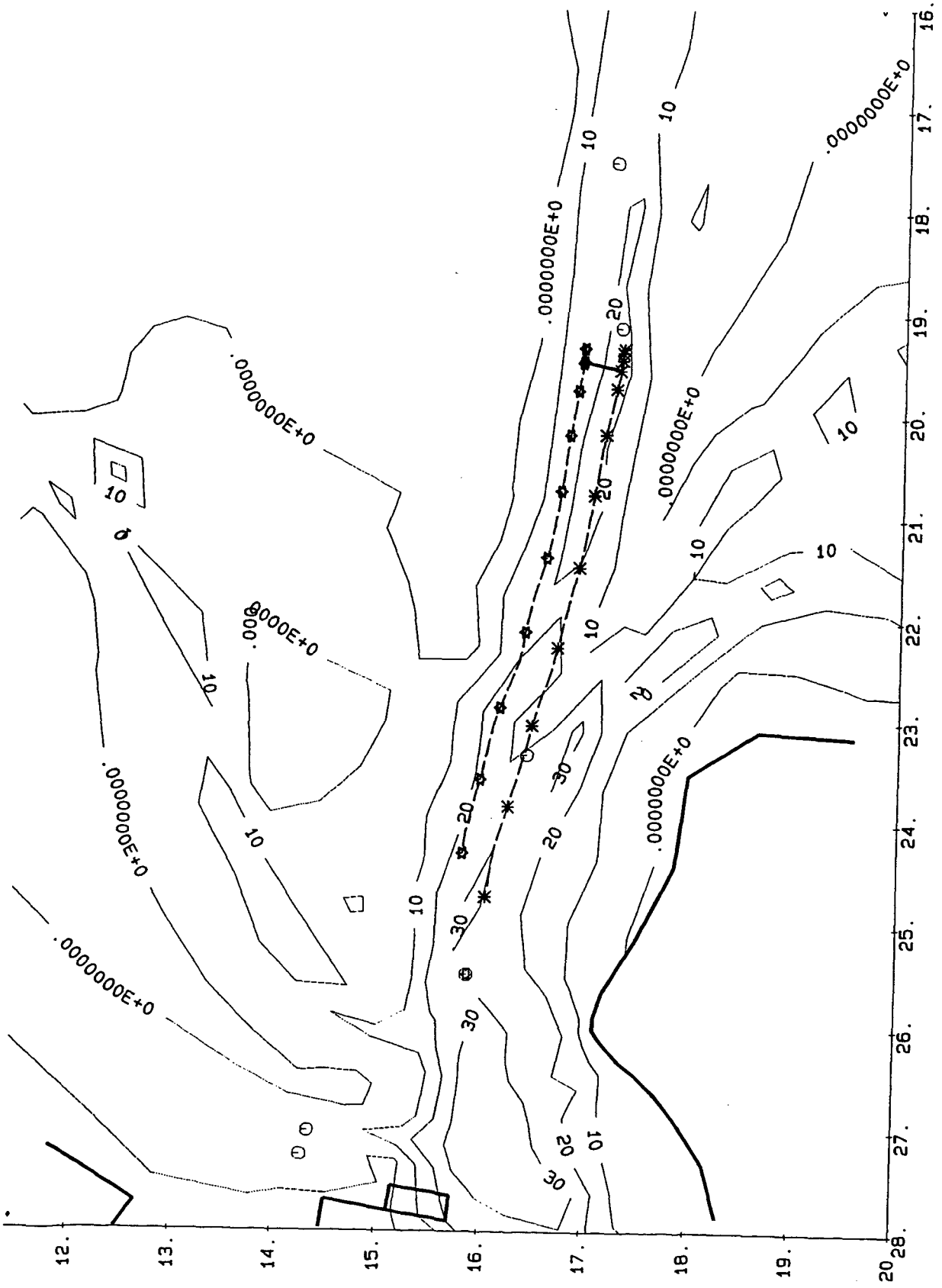

Manukau Harbour Depth, locations and trajectories Release date: 17/04/91 12:00:00 -- 14:45:00	21-12-92	043
	TRISULA	
Delft Hydraulics	z-472-20	Fig. 4.12

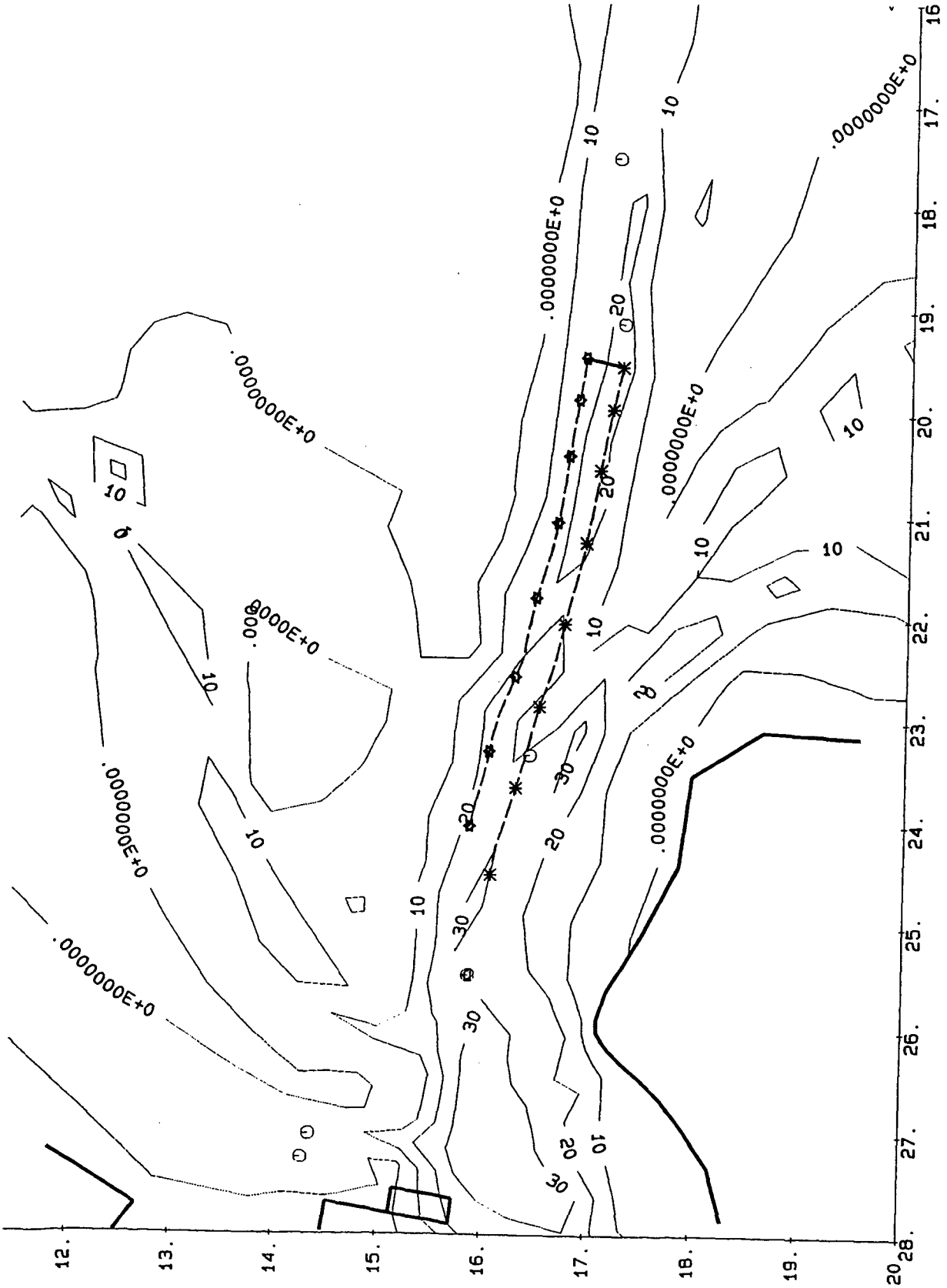

Manukau Harbour Depth, locations and trajectories Release date: 17/04/91 13:00:00 -- 14:45:00	21-12-92	043
	TRISULA	
Delft Hydraulics	z-472-20	Fig. 4.13

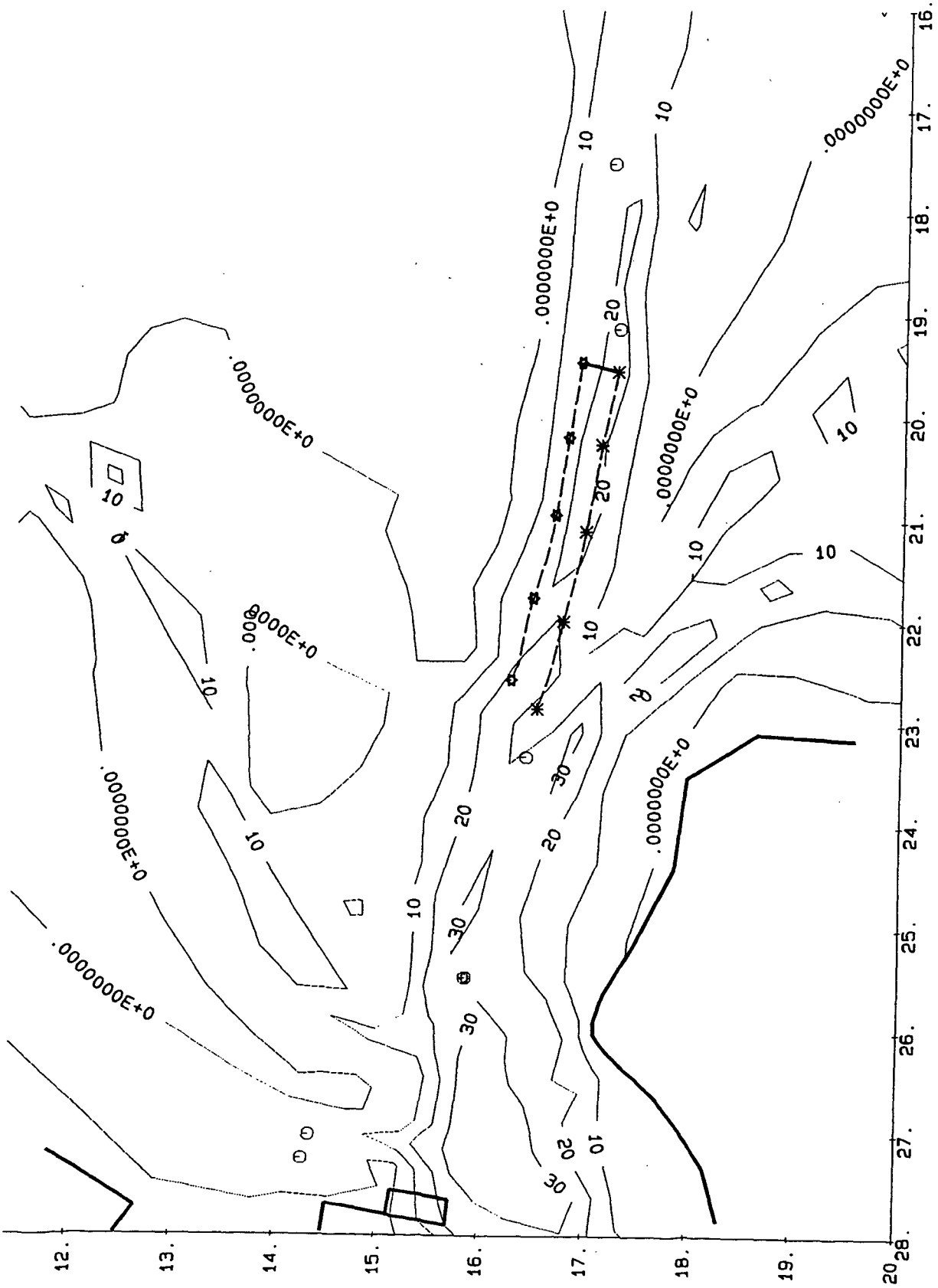

Manukau Harbour
Depth, locations and trajectories
Release date: 17/04/91 13:50:00 -- 14:50:00

21-12-92	043
TRISULA	
z-472-20	Fig. 4.14

Delft Hydraulics

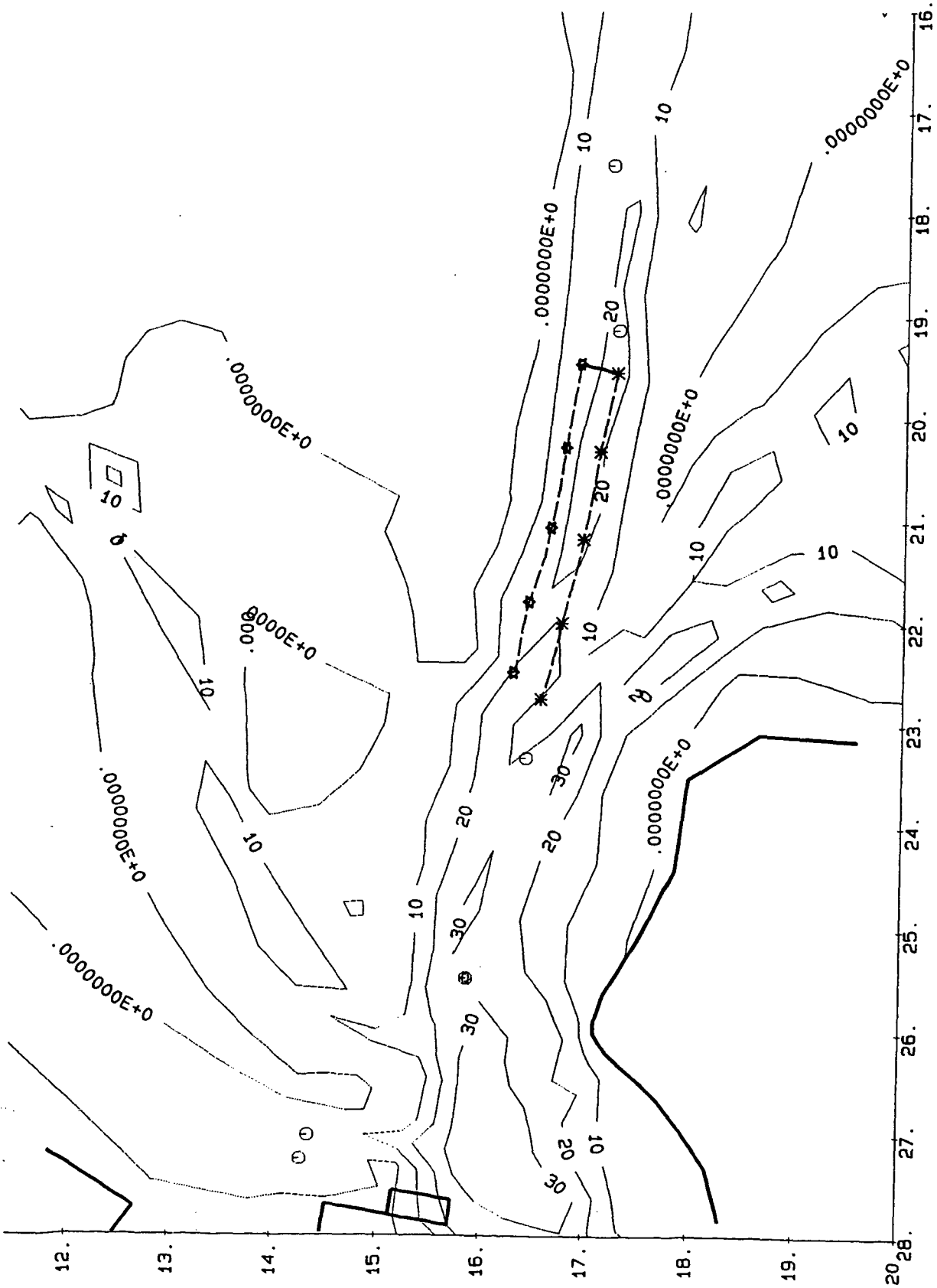

Manukau Harbour
Depth, locations and trajectories
Release date: 17/04/91 15:00:00 -- 16:00:00

21-12-92 | 043

TRISULA

Delft Hydraulics

z-472-20 | Fig. 4.15

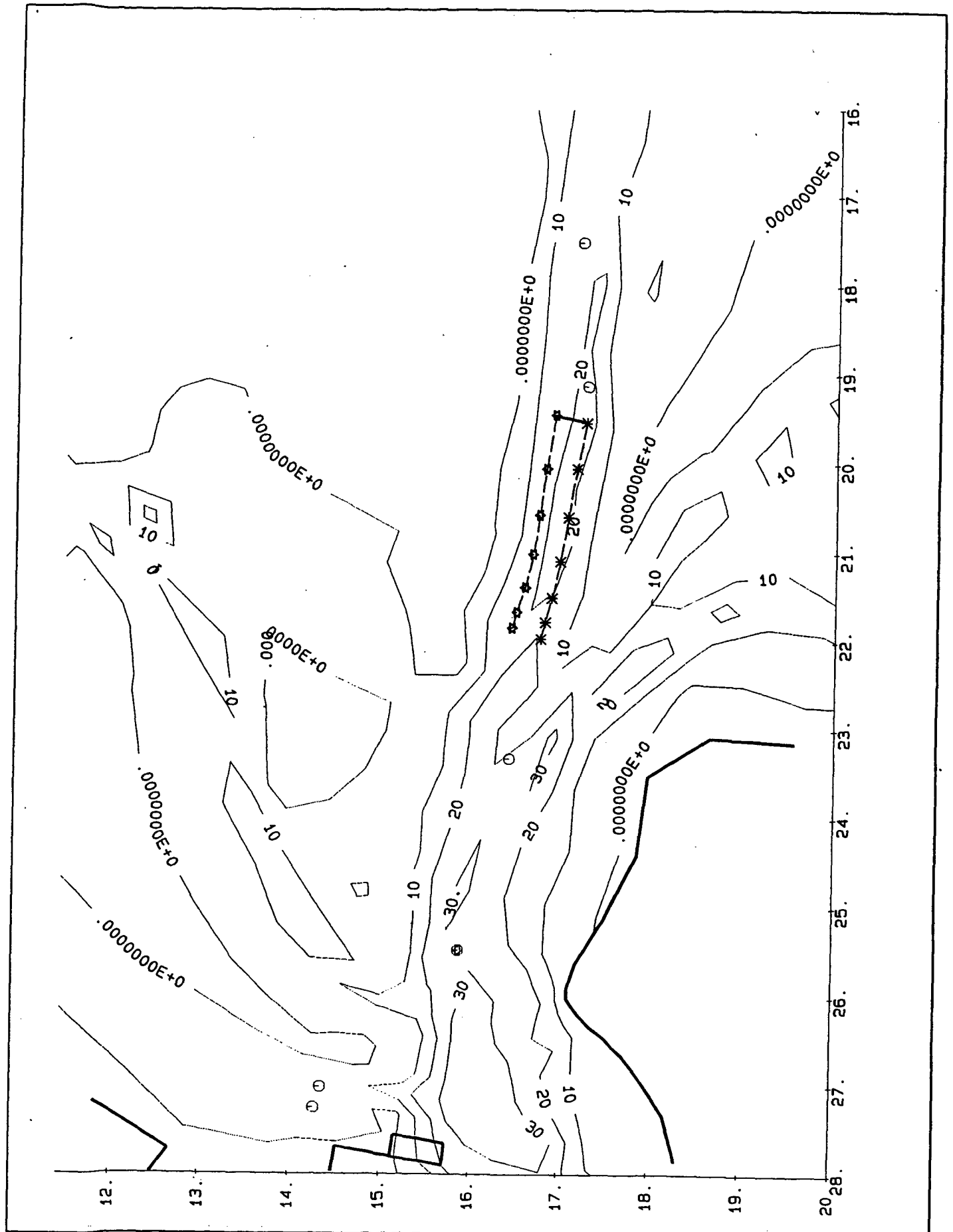

Manukau Harbour Depth, locations and trajectories Release date: 17/04/91 16:20:00 -- 17:50:00	21-12-92	043
	TRISULA	
Delft Hydraulics	z-472-20	Fig. 4.16

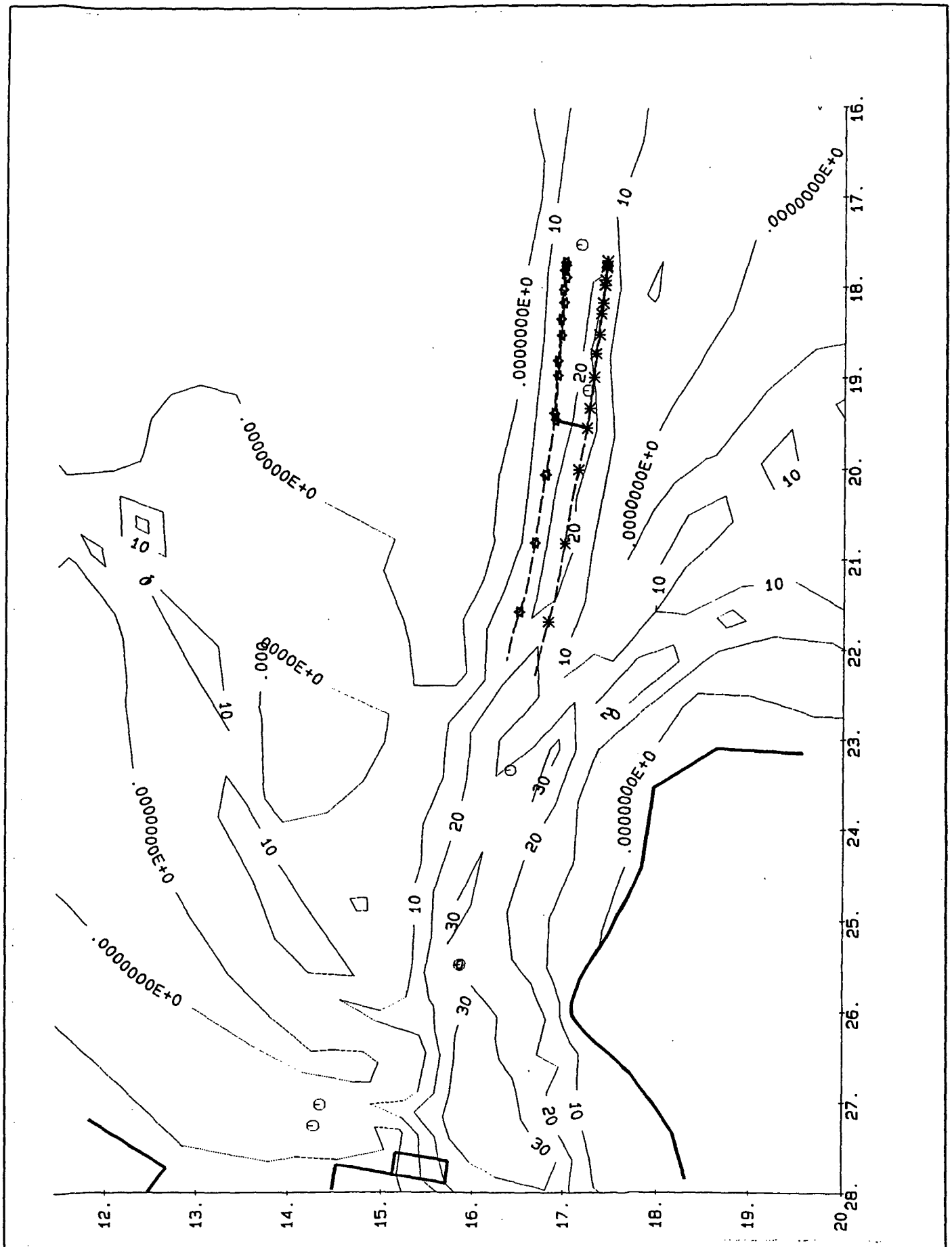

Manukau Harbour Depth, locations and trajectories Release date: 20/04/91 13:20:00 -- 17:00:00	21-12-92	043
	TRISULA	
Delft Hydraulics	z-472-20	Fig. 4.17

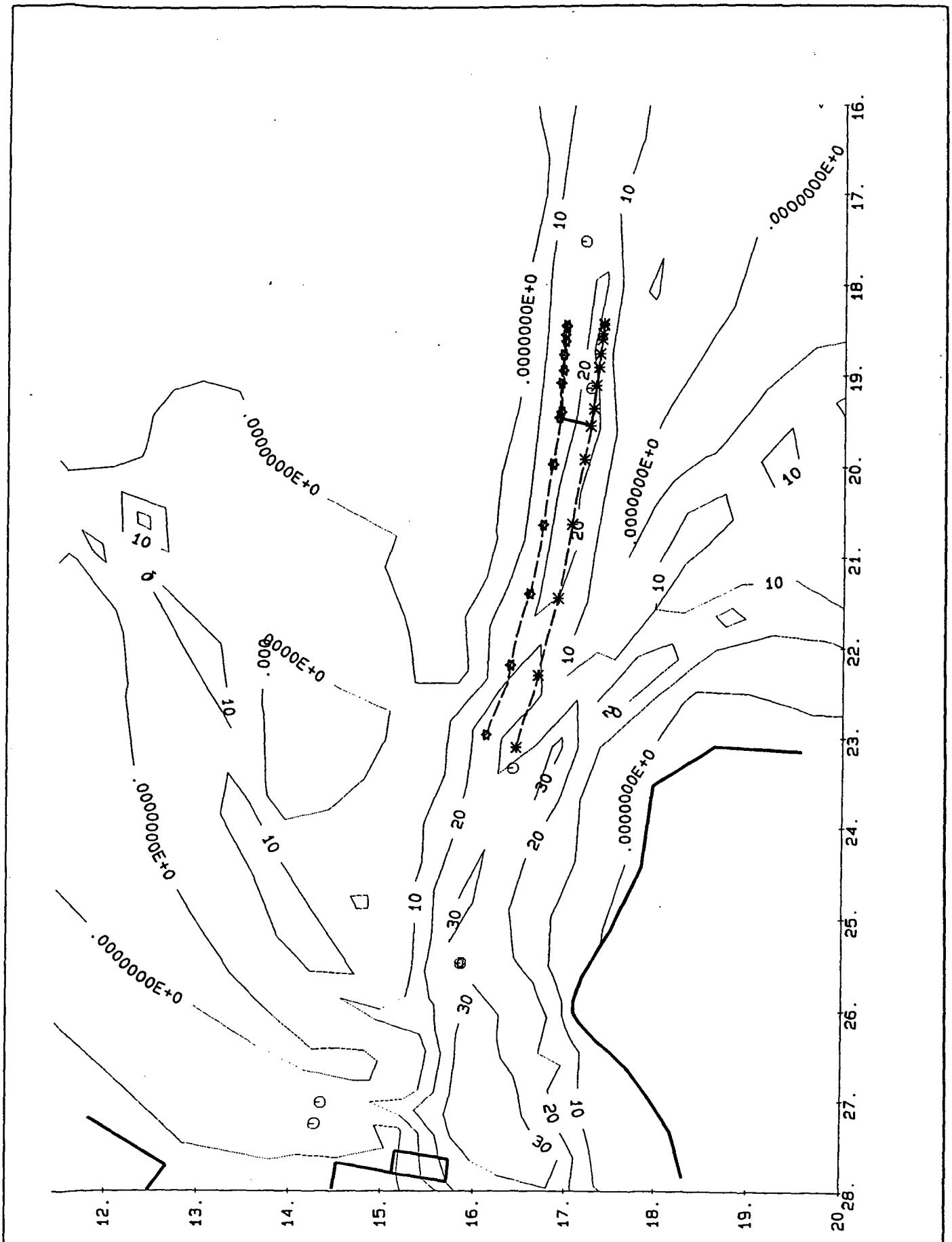

Manukau Harbour Depth, locations and trajectories Release date: 20/04/91 13:45:00 -- 17:00:00	21-12-92	043
	TRISULA	
Delft Hydraulics	z-472-20	Fig. 4.18

Appendix A

TRISULA, a simulation program for hydrodynamic flows in two and three dimensions

computer programs

TRISULA: a program for the computation of non-steady flow and transport phenomena on curvilinear co-ordinates in 2 or 3 dimensions

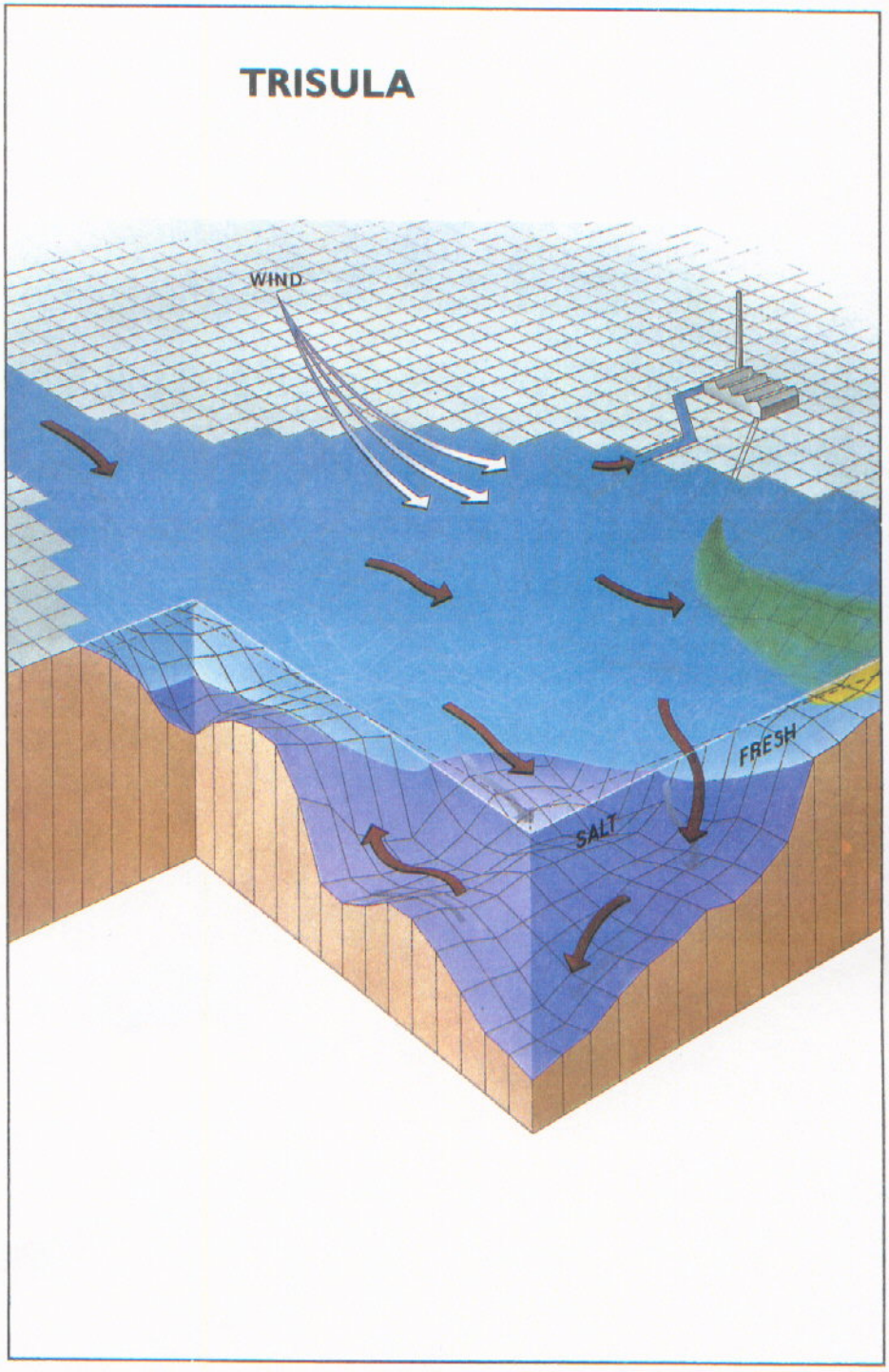

delft hydraulics

Contents

1 Introduction

Reliable information on water quantity or water quality, sediment transport and morphology can be obtained nowadays from appropriate mathematical models. In general the first step in these modelling activities concerns the simulation of the flow itself. Whether the problem is related, for example, to the stability of a hydraulic structure, to the salt intrusion or the dispersion of pollutants, or to the transport of silt and sediment, flow simulations usually form the basis of the investigations carried out.
At DELFT HYDRAULICS the program package TRISULA is available to provide the hydrodynamic basis for the water quality computations. For the steady and non-steady modelling of the far-field water quality, TRISULA is coupled with the water quality program DELWAQ. Non-steady modelling of the mid-field water quality based on the particle tracking approach is performed by coupling TRISULA to the particle tracking model DELPAR.

This document gives some background information on the concept and numerical implementation of TRISULA, and the set-up of hydrodynamic models with this program package. Further information on the practical application is found in (DELFT HYDRAULICS, 1992).

2 Conceptual description

2.1 Description of hydrodynamic system

2.1.1 Short description of TRISULA

Introduction

The multi-dimensional hydrodynamic TRISULA program package calculates non-steady flow and transport phenomena resulting from tidal and meteorological forcing. The main purpose of TRISULA is the two-dimensional (2D) and three-dimensional (3D) simulation of tidal and wind driven flow fields, including the effects of density differences due to a non-uniform temperature and salt concentration distribution (density driven flows).

Physical aspects

TRISULA solves the shallow water equations which consist of the momentum equations, the continuity equation and the transport equation. In the horizontal momentum equations the Coriolis force, density gradients, the turbulent viscosity, the shear stresses exerted by the turbulent flow on the bottom, and the wind stress are included. The vertical turbulent viscosity and diffusion are modelled by flow dependent coefficients, which are computed according to a turbulence closure technique known as the algebraic eddy-viscosity model, taking into account stable stratification through damping functions depending on the gradient Richardson number.
The horizontal turbulent exchange coefficients are the sum of a 3-D turbulence model and a 2-D sub-grid turbulence model. The magnitude of the turbulent shear stresses is based on a quadratic Chézy or Manning's formula. The wind stress is modelled by a quadratic friction law.
The vertical momentum equation is reduced to the hydrostatic pressure relation under the "shallow water assumption".
The water levels are computed together with the horizontal flow field using the continuity equation including sinks and sources.
For more detail on the governing equations and the physical aspects, see Section 2.1.2.

Applications

If the area of interest is vertically well-mixed, the depth averaged mode of TRISULA (two-dimensional simulation) is used. In this case the vertical velocity variations are not computed, and depth-mean horizontal velocities are calculated. The TRISULA 3D system is of particular interest in applications where the flow field shows significant variations in the vertical direction. This may be essential in wind driven circulation problems and partially mixed or layered flow problems. Examples are the salt intrusion in estuaries, the fresh water river discharges in bays, and the thermal stratification in lakes and seas.
Other special facilities of the TRISULA program package are:

- to account for drying and flooding of intertidal flats
- representation of narrow dams like groynes and breakwaters
- calculation of drogue tracks

- simulation of the discharge of heat and effluent, and the intake of cooling water at any location and any depth in the computational field.

2.1.2 The governing equations

Hydrodynamic equations

The three-dimensional shallow water equations and the transport equations are presented in curvi-linear orthogonal coordinates in the horizontal plane and in σ-(sigma)-coordinates in the vertical direction.

The following definitions are used:

			Units
ξ, η	:	horizontal spatial coordinates	-
σ	:	vertical coordinate ($\sigma = \frac{z-\zeta}{d+\zeta}$) (surface: $\sigma = 0$; bottom: $\sigma = -1$)	-
t	:	time	s
U, V	:	depth averaged velocities in ξ- and η-direction, defined as $U = \sum_{k=1}^{K} \Delta\sigma_k \, u_k$; $V = \sum_{k=1}^{K} \Delta\sigma_k \, v_k$	m/s
K	:	number of layers	-
u, v, ω	:	velocities in ξ-, η- and σ-direction	m/s
w	:	velocity in z-direction in the ω-σ-plane.	m/s
ζ	:	water level above some plane of reference (e.g. -5m MSL)	m
d	:	water depth below some plane of reference (e.g. -5m MSL)	m
$H=d+\zeta$	:	total water depth	m
f	:	Coriolis parameter	1/s
ν	:	eddy viscosity in ξ- and η-direction	m^2/s
$\mathcal{Z}$	:	eddy viscosity in σ-direction	m^2/s
D_h, D_v	:	eddy diffusivity in the horizontal and vertical direction	m^2/s
F_ξ, F_η	:	horizontal viscosity term	
g	:	acceleration due to gravity	m/s^2
ρ	:	water density	kg/m^3
P	:	hydrostatic water pressure	$kg/m/s^2$
P_{atm}	:	pressure at the free surface	$kg/m/s^2$
s	:	salinity	kg/m^3
T	:	temperature	C
$\sqrt{G_{\xi\xi}}$	:	distance between two consecutive coordinate lines ξ = constant, measured along the curvilinear coordinate line η = constant	m
$\sqrt{G_{\eta\eta}}$	:	distance between two consecutive coordinate lines η = constant, measured along the curvilinear coordinate line ξ = constant	m
C	:	concentration (of arbitrary scalar quantity e.g.: salinity, temperature)	
S	:	source and or sink term(s)	

Momentum equations:

$$\frac{\partial u}{\partial t} + \frac{u}{\sqrt{G_{\xi\xi}}}\frac{\partial u}{\partial \xi} + \frac{v}{\sqrt{G_{\eta\eta}}}\frac{\partial u}{\partial \eta} + \frac{\omega}{(d+\zeta)}\frac{\partial u}{\partial \sigma} + \frac{uv}{\sqrt{G_{\xi\xi}}\sqrt{G_{\eta\eta}}}\frac{\partial \sqrt{G_{\xi\xi}}}{\partial \eta} +$$

$$- \frac{vv}{\sqrt{G_{\xi\xi}}\sqrt{G_{\eta\eta}}}\frac{\partial \sqrt{G_{\eta\eta}}}{\partial \xi} - fv$$

$$= - \frac{1}{\rho\sqrt{G_{\xi\xi}}}\left(\frac{\partial P}{\partial \xi} + \frac{\partial P}{\partial \sigma}\frac{\partial \sigma}{\partial \xi}\right) + F_{\xi} + \frac{1}{(d+\zeta)^2}\frac{\partial}{\partial \sigma}\left(\Xi \frac{\partial u}{\partial \sigma}\right)$$

and

$$\frac{\partial v}{\partial t} + \frac{u}{\sqrt{G_{\xi\xi}}}\frac{\partial v}{\partial \xi} + \frac{v}{\sqrt{G_{\eta\eta}}}\frac{\partial v}{\partial \eta} + \frac{\omega}{(d+\zeta)}\frac{\partial v}{\partial \sigma} + \frac{uv}{\sqrt{G_{\xi\xi}}\sqrt{G_{\eta\eta}}}\frac{\partial \sqrt{G_{\eta\eta}}}{\partial \xi} +$$

$$- \frac{uu}{\sqrt{G_{\xi\xi}}\sqrt{G_{\eta\eta}}}\frac{\partial \sqrt{G_{\xi\xi}}}{\partial \eta} + fu$$

$$= - \frac{1}{\rho\sqrt{G_{\eta\eta}}}\left(\frac{\partial P}{\partial \eta} + \frac{\partial P}{\partial \sigma}\frac{\partial \sigma}{\partial \eta}\right) + F_{\eta} + \frac{1}{(d+\zeta)^2}\frac{\partial}{\partial \sigma}\left(\Xi \frac{\partial v}{\partial \sigma}\right)$$

Under the "shallow water approximation" (see Section 3.2) the vertical momentum equation is reduced to the hydrostatic pressure relation, which gives after integration :

$$P = P_{atm} + gH \int_{\sigma}^{o} \rho(\xi,\eta,\sigma',t)d\sigma'$$

The pressure gradient is expressed as:

$$\frac{g}{\sqrt{G_{\xi\xi}}}\frac{\partial \zeta}{\partial \xi} + g\frac{(d+\zeta)}{\rho\sqrt{G_{\xi\xi}}}\int_{\sigma}^{0}\left(\frac{\partial \rho}{\partial \xi} + \frac{\partial \sigma}{\partial \xi}\frac{\partial \rho}{\partial \sigma}\right)d\sigma'$$

and

$$\frac{g}{\sqrt{G_{\eta\eta}}}\frac{\partial\zeta}{\partial\eta} + g\frac{(d+\zeta)}{\rho\sqrt{G_{\eta\eta}}}\int_{\sigma}^{0}\left(\frac{\partial\rho}{\partial\eta} + \frac{\partial\sigma}{\partial\eta}\frac{\partial\rho}{\partial\sigma}\right)d\sigma'$$

For water of constant density, the pressure terms reduce to:

$$\frac{g}{\sqrt{G_{\xi\xi}}}\frac{\partial\zeta}{\partial\xi}$$

$$\frac{g}{\sqrt{G_{\eta\eta}}}\frac{\partial\zeta}{\partial\eta}$$

For 3D computations the divergence of the turbulent momentum fluxes (Reynold stresses) are based and implemented on a non-equidistant rectangular grid in the horizontal:

$$F_{\xi} = \frac{1}{\sqrt{G_{\xi\xi}}}\frac{\partial\tau_{\xi\xi}}{\partial\xi} + \frac{1}{\sqrt{G_{\eta\eta}}}\frac{\partial\tau_{\xi\eta}}{\partial\eta}$$

$$F_{\eta} = \frac{1}{\sqrt{G_{\xi\xi}}}\frac{\partial\tau_{\eta\xi}}{\partial\xi} + \frac{1}{\sqrt{G_{\eta\eta}}}\frac{\partial\tau_{\eta\eta}}{\partial\eta}$$

with:

$$\tau_{\xi\xi} = \frac{2\nu}{\sqrt{G_{\xi\xi}}}\left(\frac{\partial u}{\partial\xi} + \frac{\partial u}{\partial\sigma}\frac{\partial\sigma}{\partial\xi}\right)$$

$$\tau_{\xi\eta} = \tau_{\eta\xi} = \nu\left(\frac{1}{\sqrt{G_{\eta\eta}}}\left(\frac{\partial u}{\partial\eta} + \frac{\partial u}{\partial\sigma}\frac{\partial\sigma}{\partial\eta}\right) + \frac{1}{\sqrt{G_{\xi\xi}}}\left(\frac{\partial v}{\partial\xi} + \frac{\partial v}{\partial\sigma}\frac{\partial\sigma}{\partial\xi}\right)\right)$$

$$\tau_{\eta\eta} = \frac{2\nu}{\sqrt{G_{\eta\eta}}}\left(\frac{\partial v}{\partial\eta} + \frac{\partial v}{\partial\sigma}\frac{\partial\sigma}{\partial\eta}\right)$$

The turbulent momentum fluxes can be regarded as second order effects relative to the material derivative of the mean velocity. Despite the lack of curvature terms, the implementation of the Reynold stresses is also accurate for moderately curved horizontal grids. Only third order errors are introduced.
For more details, see (Uittenbogaard et al., 1992).

For depth averaged flow computations and large scale circulation on coarse grids, the horizontal viscosity terms are simplified according to:

$$F_\xi = \nu \left(\frac{1}{\sqrt{G_{\xi\xi}}\sqrt{G_{\xi\xi}}} \frac{\partial^2 u}{\partial \xi^2} + \frac{1}{\sqrt{G_{\eta\eta}}\sqrt{G_{\eta\eta}}} \frac{\partial^2 u}{\partial \eta^2}\right)$$

$$F_\eta = \nu \left(\frac{1}{\sqrt{G_{\xi\xi}}\sqrt{G_{\xi\xi}}} \frac{\partial^2 v}{\partial \xi^2} + \frac{1}{\sqrt{G_{\eta\eta}}\sqrt{G_{\eta\eta}}} \frac{\partial^2 v}{\partial \eta^2}\right)$$

Continuity equation:

$$\frac{\partial \zeta}{\partial t} + \frac{1}{\sqrt{G_{\xi\xi}}\sqrt{G_{\eta\eta}}} \frac{\partial[(d+\zeta)u\sqrt{G_{\eta\eta}}]}{\partial \xi} + \frac{1}{\sqrt{G_{\xi\xi}}\sqrt{G_{\eta\eta}}} \frac{\partial[(d+\zeta)v\sqrt{G_{\xi\xi}}]}{\partial \eta} + \frac{\partial \omega}{\partial \sigma} = 0$$

The ω-(omega)-velocity in σ-direction is defined as

$$\omega = w - \frac{1}{\sqrt{G_{\xi\xi}}\sqrt{G_{\eta\eta}}} \left[u\sqrt{G_{\eta\eta}} \left(\sigma \frac{\partial H}{\partial \xi} + \frac{\partial \zeta}{\partial \xi}\right) + v\sqrt{G_{\xi\xi}} \left(\sigma \frac{\partial H}{\partial \eta} + \frac{\partial \zeta}{\partial \eta}\right) \right] - \left(\sigma \frac{\partial H}{\partial t} + \frac{\partial \zeta}{\partial t}\right)$$

Transport equation:

$$\frac{\partial[(d+\zeta)C]}{\partial t} + \frac{1}{\sqrt{G_{\xi\xi}}\sqrt{G_{\eta\eta}}} \left[\frac{\partial[(d+\zeta)u\sqrt{G_{\eta\eta}}C]}{\partial \xi} + \frac{\partial[(d+\zeta)v\sqrt{G_{\xi\xi}}C]}{\partial \eta}\right] +$$

$$\frac{\partial(\omega C)}{\partial \sigma} = \frac{1}{(d+\zeta)} \left[\frac{\partial}{\partial \sigma} D_v \cdot \frac{\partial C}{\partial \sigma}\right] +$$

$$\frac{(d+\zeta)}{\sqrt{G_{\xi\xi}}\sqrt{G_{\eta\eta}}} \left\{\frac{\partial}{\partial \xi} \left[D_h \cdot \frac{\sqrt{G_{\eta\eta}}}{\sqrt{G_{\xi\xi}}} \cdot \frac{\partial C}{\partial \xi}\right] + \frac{\partial}{\partial \eta} \left[D_h \cdot \frac{\sqrt{G_{\xi\xi}}}{\sqrt{G_{\eta\eta}}} \cdot \frac{\partial C}{\partial \eta}\right]\right\} + (d+\zeta).S$$

Boundary conditions at the surface and at the bottom

The boundary conditions at the surface and at the bottom for the continuity equation are given by:

$\omega(0) = \omega(1) = 0$

At the surface and at the bottom the boundary conditions for the momentum equations are successively:

$$\frac{\nu}{H}\frac{\partial u}{\partial \sigma} = \frac{\tau_{bottom_\xi}}{\rho}, \quad for\ \sigma = -1$$

$$\frac{\nu}{H}\frac{\partial u}{\partial \sigma} = \frac{\tau_{wind_\xi}}{\rho}, \quad for\ \sigma = 0$$

$$\frac{\nu}{H}\frac{\partial v}{\partial \sigma} = \frac{\tau_{bottom_\eta}}{\rho}, \quad for\ \sigma = -1$$

$$\frac{\nu}{H}\frac{\partial v}{\partial \sigma} = \frac{\tau_{wind_\eta}}{\rho}, \quad for\ \sigma = 0$$

For the formulations of the bed stress and the wind stress, see the subsection below.

Physical aspects

Turbulence closure

For the vertical eddy viscosity and eddy diffusivity three levels of turbulence closure are implemented:

- an Algebraic eddy viscosity model (no transport equation)
- a k-L turbulence model (one transport equation for k)
- the k-ϵ turbulence model (two transport equations for k and ϵ).

For 3D computations in the present release, the algebraic turbulence model is simple, robust and efficient. The use of this model is restricted to the computation of water levels and velocity profiles in weakly stratified flows, see (Uittenbogaard et al., 1992).

The algebraic model implemented in TRISULA is a combination of two models.
In both models the mixing length as well as the vertical profile of the turbulent kinetic energy are prescribed. In the first model the turbulent kinetic energy is completely determined by its flow dependent extremes near the bottom and the free surface:

$$k_1 = C\,[u_*^b]^2\,[1-\frac{(z+d)}{H}] + C\,[u_*^w]^2\,\frac{(z+d)}{H}$$

with C = 3.3, a calibration constant derived from the C_μ of the k-ϵ model.

For robustness the friction velocity is computed following:

$$u_*^b = MAX(\frac{1}{K}\sum_{k=1}^{K} u_*(k),\ u_*(K))$$

In the second model the turbulent kinetic energy is computed from a local equilibrium between production and dissipation:

$$k_2 = C \,.\, L^2 \,.\, \{(\frac{\partial u}{\partial z})^2 + (\frac{\partial v}{\partial z})^2\}$$

The mixing length L is prescribed as a function of the flow geometry only, for which the so-called Bakhmetev-profile is used. For a stably stratified flow the mixing length L is reduced or "damped", depending on the gradient Richardson number (Simonin et. al., 1989). The relation for the mixing length now reads:

$$L = \kappa\,[z+d] \,.\, [1-\frac{(z+d)}{H}]^{\frac{1}{2}} \,.\, F_L(Ri)$$

with

κ = 0.41, the Von Karman constant
$F_L(Ri)$ = the damping function

The gradient Richardson number Ri is defined as (Richardson, 1920; Taylor, 1931; Miles, 1987):

$$Ri = -\frac{g}{\rho}.\frac{\frac{\partial \rho}{\partial z}}{(\frac{\partial u}{\partial z})^2+(\frac{\partial v}{\partial z})^2}$$

The vertical eddy viscosity is founded on the Kolmogorov-Prandtl eddy viscosity concept (Kolmogorov, 1942; Prandtl, 1945) given by

$$\nu^{3D} = C_\mu' . L . \sqrt{k}$$

with constant C_μ' to be calibrated.

The second algebraic model gives no vertical mixing in the case of wind at the layer interface where the velocity gradient is zero. Therefore the first and second model are combined in the following way:

$$\Xi^{3D} = C_{\mu}' L \sqrt{\max(k_1, k_2)}$$

The vertical eddy diffusivity is defined as:

$$D_V^{3D} = \frac{\Xi^{3D}}{\sigma_\chi . F_\sigma(Ri)}$$

with the turbulent Prandtl/Schmidt number for constituent and F a damping function (Munk-Anderson, 1948).

In the horizontal direction the eddy viscosity and eddy diffusivity are the sum of a 3D turbulence model and a 2D sub-grid turbulence model. Sub-grid models are subject of further study. Therefore in the present release the user must specify a constant value or specify the distribution over the model grid.
For a detailed discussion on the implementation of the turbulence closure applied in TRISULA we refer to (Uittenbogaard et al. 1992).

The bed stress formulation

For the depth averaged flow (2DH) the magnitude of the shear stresses exerted by the turbulent flow on the bottom is determined by U_{tot} being the magnitude of the depth averaged horizontal velocity vector:

$$\frac{|\tau|}{\rho_0} = \frac{g}{C_{2D}^{\ 2}} * U_{tot}^{\ 2}$$

with

$U_{tot} = U^2 + V^2$

The 2D-friction coefficient C_{2D} is computed following the bed stress formulation selected by the user. There are in principle three options available:

- Chezy formulation
  This is a rather straight formulation as:
  C_{2D} = Chezy coefficient

- Manning's formulation
  $C_{2D} = H^{1/6}/n$
  with: H = total water depth
  n = Manning's coefficient

- White Colebrook's formulation
  $C_{2D} = 18.0 * {}^{10}\log(12.0 * H/k)$
  with: H = total water depth
  k = White Colebrook's coefficient

For the 3D computations the bottom shear stress is related to the velocity in the bottom layer (k = K) using an equivalent C_{3D} of the 2DH bottom friction coefficient C_{2D}.

$$\frac{|\tau|}{\rho_0} = \frac{g}{C_{3D}^2} * (U_{tot}^2)_K$$

with

$$(u_{tot})_K = u^2_K + v^2_K$$

However, the coefficient C_{3D} is based on the velocity of the computational bottom layer and it is determined from the assumption that the velocity profile near the bottom follows the so-called 'logarithmic law' for the flow along smooth and rough bottoms.

The 3D-friction coefficient C_{3D} for a rough wall is computed at the first grid points nearest to the bottom. TRISULA offers two options to compute C_{3D}:

a. Roughness-concept:

From the 'logarithmic law' for flow along a rough bottom, with roughness height z_0, it follows that

$$C_{3D} = \frac{\log(\frac{\Delta\sigma_K * H}{z_0})}{\kappa}$$

The bottom roughness coefficient z_0 [in meters] must be prescribed by the user.

b. Chezy-concept:

The 3D-computations may be preceded by 2DH-computations for which C_{2D} is calibrated in each u- and v- velocity point or the user has experience in estimating C_{2D}. Therefore, TRISULA provides the possibility to use the 2DH bed stress coefficients to compute an equivalent roughness coefficient as follows:

$$z_0 = H \exp[-(1+\frac{\kappa}{\sqrt{g}}C_{2D})]$$

This relation is valid under the assumption of the logarithmic profile and provided stresses or dissipation in 2DH-computations are equal to 3D-computations.

For a thorough discussion on these matters see (Uittenboogaard et. al., 1992).

The wind stress formulation

The surface may be forced by the wind stress vector usually related to the ensemble averaged wind speed U_{10}, measured 10 m above the mean free surface, as:

$$|\tau| = \rho_{air} C_D U_{10}^2$$

with ρ_{air} is the air density.

The air density ρ_{air} and the wind drag coefficient C_D in TRISULA are user defined input parameters.

Equation of state

The density of water ρ is a function of salinity (s) and temperature (T). In TRISULA the empirical relation given by Eckart (1958) is used:

$$\rho = \frac{1000\ P_0}{(\lambda + \alpha_0 P_0)}$$

with:

$$\lambda = 1779.5 + 11.25\ T - 0.0745\ T^2 - (3.80 + 0.01\ T)\ s$$

$$\alpha_0 = 0.6980$$

$$P_0 = 5890 + 38\ T - 0.375\ T^2 + 3\ s$$

2.1.3 The hydrodynamic model

Computational grid and bathymetry schematization

The area to be modelled can be covered with a rectangular or curvi-linear, orthogonal grid. In general a curvi-linear grid is chosen because complicated irregular geometries can be modelled more accurately. The grid cells will have a high resolution in the areas of interest, i.e. along the coast, and get coarser towards the open model boundaries offshore. Thus the computational efficiency will be increased. This approach implies too, that bathymetries can be refined in local areas of interest, because to every grid cell a depth value is attached. However, if the bathymetric information is insufficient to justify such a high resolution, the resolution is limited and adapted to the data available.

Initial and boundary conditions

To solve the shallow water equations, TRISULA needs initial and boundary conditions. In general, lacking realistic secure information, both the horizontal velocity components and the derivative of the water level in x and y direction initially are taken zero. Concerning the boundary conditions at the closed boundaries the velocity normal to the boundary is set zero. At the open boundaries, either a water level or a (normal) velocity or a flux can be prescribed. The choice depends on the problem to solve. In general, boundary conditions are obtained from available measurements, from the results of an overall model and from available literature.

Physical and geometrical aspects

Most physical processes like wind stress at the surface and turbulent shear stress at the bottom, are modelled leaving the user with a set of physical parameters (i.e. Manning or Chezy coefficient, wind drag coefficient, density of water and air) for which a suitable estimate of the magnitude has to be made. In general the magnitude of these parameters is varied in several simulation runs to investigate their influence on the model performance. Furthermore, TRISULA accounts for drying and flooding at intertidal flats.

2.2 Assumptions with respect to the hydrodynamic system

During the development of the hydrodynamic TRISULA program package, the following assumptions have been made. The vertical velocity is assumed to be small and the vertical acceleration is assumed to be neglectable compared to the gravitational accelaration. Together these assumptions are also known as the "shallow water assumption" which imposes two restrictions on the applicability of TRISULA:

- vertical accelerations due to buoyancy effects cannot be taken into account properly
- sudden variations in the bottom topography cannot be reproduced correctly.

Furthermore, in the derivation of the equations of motion that are modelled by TRISULA, the Boussinesq approximation has been applied. In the Boussinesq approximation the fluid is taken to be incompressible and density variations are neglected everywhere, except in the buoyancy term.

3 Algorithmic implementation

3.1 Algorithmic implementation of the hydrodynamic system

In this section the numerical aspects and the solution method used in TRISULA are described. Futhermore the general set-up of the hydrodynamic model, i.e. the generation of the bathymetric schematization, the boundary conditions and the description of some physical parameters are given.

3.1.1 Numerical aspects of TRISULA

The horizontal staggered grid model

For the discretization in space a staggered grid is used. The water level points are situated in the centre of a continuity cell, whereas the normal velocity components are located at the boundaries of this cell, see Figure 3.1.1 below. Staggered grids are advantageous because the implementation of boundary conditions becomes simple, the number of computational values is decreased while maintaining the same accuracy and spatial oscillations in the waterlevels are excluded, see Stelling (1984).

The vertical grid

The vertical grid consists of layers determined by a fixed number of permeable interfaces. As a result of the use of the so-called σ-transformation for the vertical coordinate, the number of layers is constant over the entire computational field (see Figure 3.1.2 below). This leads to a smooth representation of the topography, giving the same order of vertical resolution for the shallow and deeper parts of the water. The vertical grids may have a non-equidistant distribution, which allows a more detailed reproduction of features in zones of particular interest, e.g. in the top (heat exchange) and or bottom (sediment transport).

The solution method for the equations of motion

The coupling of the vertical layers exists by means of vertical advection and diffusion (turbulent shear stresses). The sigma coordinate system leads to very thin layers in the shallow areas. To prevent instabilities due to the vertical diffusion term this term is treated fully implicitly. This leads to a tri-diagonal system of equations in the vertical. The layer velocities are expressed in the waterlevels by a double sweep. The layer velocities are substituted in the depth averaged continuity equation. The equations for the waterlevels are solved with an Alternating Direction Implicit (A.D.I.) method reported in Stelling (1984).

For the waterlevels only tri-diagonal systems of equations along grid lines need to be solved while maintaining second order accuracy in space and time. The layer velocities are computed from the waterlevels. In the intermediate timestep when the pressure term is taken explicitly, the horizontal advection terms are solved implicitly using a Point Jacobi iterative scheme.

The advection terms

For the time integration of the advection terms, two different approximations are used in succession, an implicit higher order upwind approximation followed by an explicit second order central approximation. The resulting finite difference scheme for the complete timestep is second order accurate. Spatial oscillations in the velocities are prevented by introducing fourth order dissipation, Stelling (1984) and Stelling and Leendertse (1991).

The horizontal viscosity terms

In Section 2.2 the horizontal turbulent momentum fluxes are described. For the depth averaged flow computations the horizontal viscosity terms are simplified, see Section 2.2. The simplified horizontal viscosity term contains only second derivatives of the u-velocity and is integrated fully implicitly. This is unconditionally stable.

For 3D small scale computations the complete Reynold stress tensor is implemented. The shear stress $\tau_{\xi\eta}$ in the u-momentum equation contains derivatives of the v-velocity. Therefore the Reynold stresses are integrated explicitly. This leads to the following stability condition:

$$\Delta t \leq \frac{1}{2\nu}\left(\frac{1}{\sqrt{G_{\xi\xi}}^{\,2}}+\frac{1}{\sqrt{G_{\eta\eta}}^{\,2}}\right)^{-1}$$

Accuracy wave propagation

The time integration method for the waterlevels is of the ADI type. This means that waterlevels and velocities are implicitly solved along grid lines.

The wave propagation is connected with the Courant number, defined for a staggered orthogonal curvilinear grid as:

$$Cf = 2\Delta t\sqrt{gH}\left(\frac{1}{\sqrt{G_{\xi\xi}}^{\,2}}+\frac{1}{\sqrt{G_{\eta\eta}}^{\,2}}\right)^{\frac{1}{2}}$$

For a large timestep, Courant number larger than $4\sqrt{2}$,in combination with an irregular geometry (islands, channels), which does not follow the gridlines, the flow pattern is badly represented, Stelling (1984).

The solution method for the equation of transport

The transport equation is solved for each half time step, after computation of the water levels and the vertical velocities. To insure that the total mass is conserved the transport equation is solved in its flux form. The time integration follows the integration procedure for the continuity equation and combines an A.D.I scheme in the horizontal direction with a fully implicit scheme in the vertical direction, Stelling (1984) and Stelling and Leendertse (1991). The equations are solved by an iterative Point Jacobi method to decouple the horizontal and vertical direction.

For the horizontal advection terms, a finite difference scheme is used that conserves large gradients and higher derivatives without generating spurious oscillations. To avoid negative concentrations a so-called Forester-filter, a local diffusion operator, Forester (1979), is used. The horizontal diffusion is implemented fully implicitly along sigma planes.

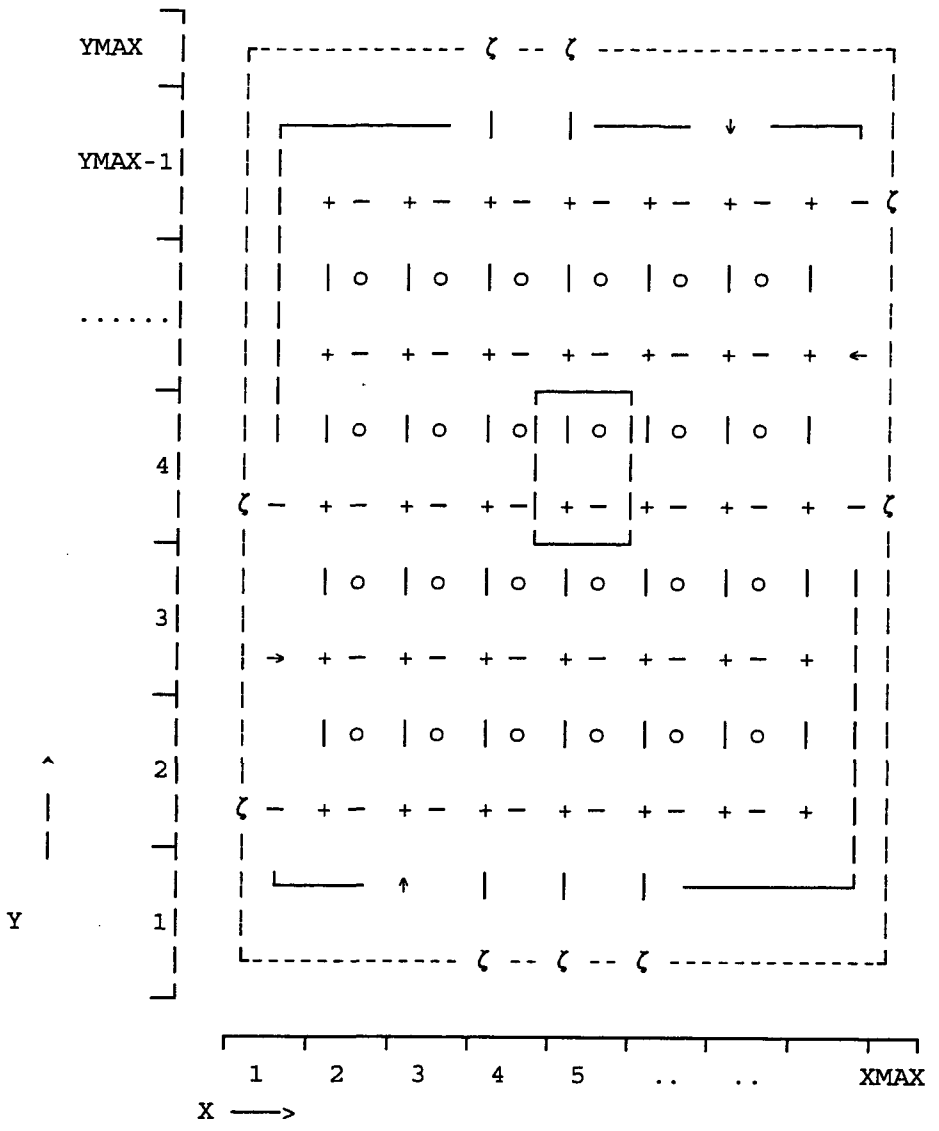

Default computational grid with arbitrary openings Figure 3.1.1

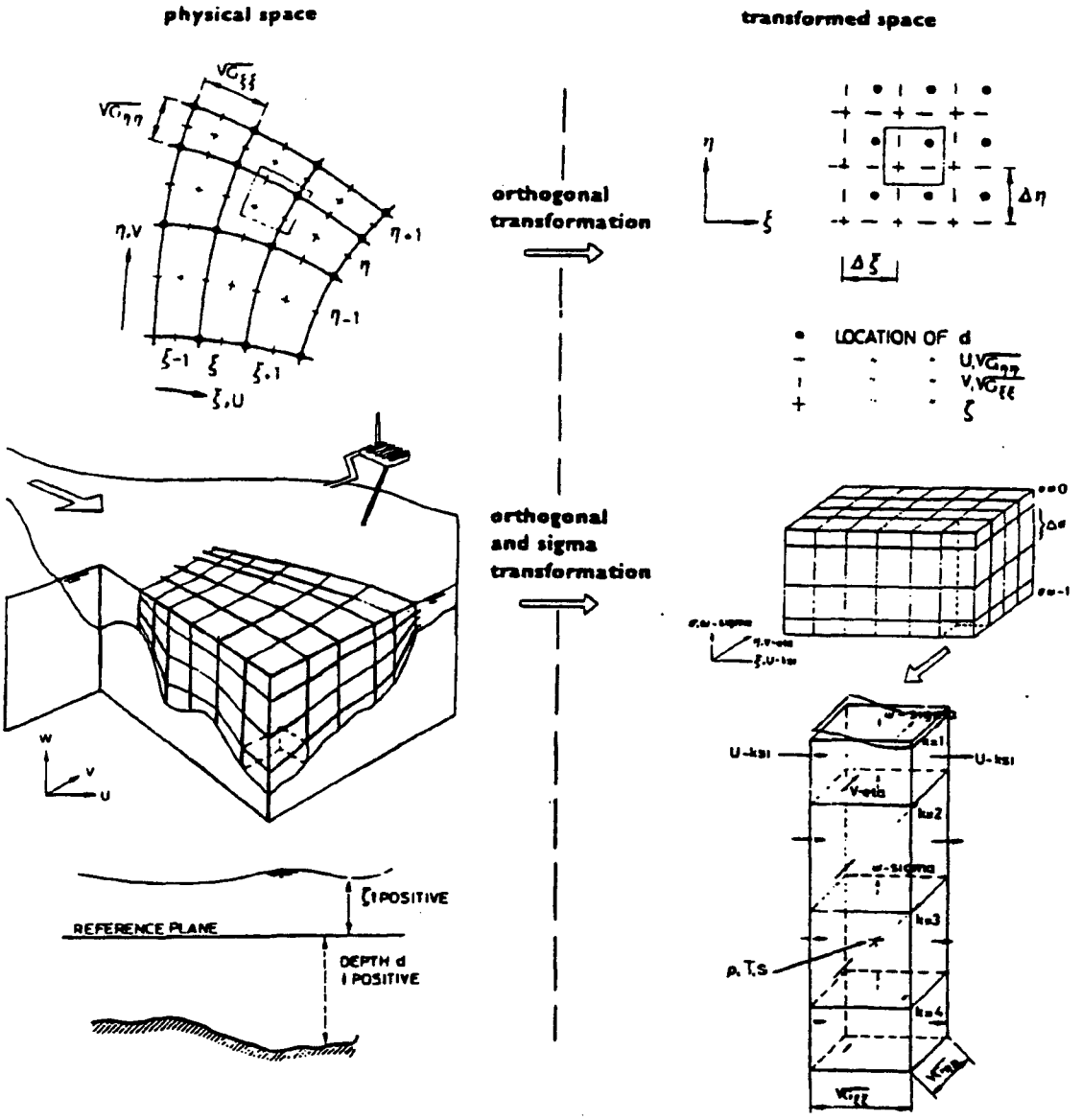

Orthogonal and Sigma transformation

Figure 3.1.2

Drying and flooding procedure on tidal flats

During computation of the flow, drying and flooding checks are performed. At the beginning of every sweep through a row of cells the local water depth at the velocity points is checked. If the water depth is above a uniform threshold VAR, the velocity point becomes active if it was inactive. After the computation of the water levels, the local water depth defined by the difference between the water level and the mean depth is checked at every water level point. If the local water depth is below the drying threshold 1/2 VAR, the velocity points around the water level points are inactivated and the continuity equation is solved again. This sophisticated method has proved indispensable for areas with large tidal flats.

3.1.2 Implementation of the hydrodynamic model

Setting up of a TRISULA hydrodynamic model mainly consists of the following subtasks:

- construction of a orthogonal curvi-linear grid
- schematization of bathymetric information
- prescription of boundary conditions
- definition of physical and numerical parameters
- introduction of check-stations, special hydraulic constructions etc.
- collection and processing of data.

Each of these items will be discussed below.

Generation of the Computational grid

The TRISULA hydrodynamics package allows for the application of orthogonal curvilinear grids in modelling a certain area. There are two main reasons for the application of a curvilinear grid:

- Computational effort can be minimized by definition of a high grid resolution in areas of interest in combination with low grid resolutions far away, for example near model boundaries.
- The notorious representation of coastlines by staircase boundaries, which introduces artificial viscosity in the calculations, can be avoided by curving the gridlines parallel to the coastal boundary.

Construction of a suitable curvilinear grid is not a simple task, since a grid must not only possess the characteristics mentioned above, but also has to satisfy two restrictions of numerical nature. These restrictions are:

- Grid lines must intersect perpendicularly (orthogonal grid), to provide a computationally more efficient code for the hydrodynamics solver.
- Grid spacings must vary smoothly over the computational region, to minimize inaccuracy errors in the finite difference operators.

The actual construction of a grid is realized in an iterative procedure, that allows for a

stepwise definition of the model grid, working from a coarse version of the grid to finer versions until the final resolution is achieved. DELFT HYDRAULICS applies a graphical interactive program that allows a user to manipulate each of the intermediate grids in order to obtain the desired resolution and shape. Repetitive calls of the orthogonalisation procedure provides full orthogonality for the final grid. The grid refinement module is designed in such a way, that grid smoothness is an intrinsic property of the final grid.

The general grid layout and the size of the grid is chosen in accordance with the specific aim of the modelling study. Many considerations have to be taken into account, which we cannot cover in this context. However, the location of the model boundaries and type of boundary conditions, which are very important for succesful modelling, will be detailed after the next section.

Generation of the Bathymetry schematization

The task of assigning depth values to gridpoints can be separated in two main components. The first one is the gathering of the raw bathymetric data, the second one is the actual interpolation of these raw data on the structured grid.
The bathymetric data can be obtained by:

- digitizing Bathymetric charts (Admirality Charts, Fair Sheets)
- extracting the bottom schematization of the area to be modelled from the bottom schematization of an overall coarser hydrodynamic model
- using available measurements (echo-soundings).

These possibilities can be combined to obtain the most elaborate depth data. However, care must be taken when depth data originating from different sources are combined. Special attention must be given to the reference levels, which may not be the same. In that case corrections are necessary to ensure that all depth values refer to only one reference level. The combined bathymetric data may not all be of the same resolution, nor of the same quality with respect to accuracy or recentness, nor may they cover the complete area of the grid. If all data are simply stacked into one file, the problem arises that high quality data becomes contaminated with low quality data, thus spoiling interpolation results that might have been good if properly dealt with. So, one must carefully evaluate the quality of the various bathymetric datasets, before the decision is made to include it or discard it.

The interpolation of these data to the points of the grid should supply a bathymetry that resembles the natural bathymetry as closely as possible. However, this does not mean that the best bathymetry is obtained by always assigning the actual waterdepths to all gridpoints. Since TRISULA calculates averaged flow velocities and waterheights, equality of averaged bathymetric features is more important than equality of bathymetric features at discrete grid positions. Therefore, we adopt a volume preserving interpolation method that utilises all datapoints if there is redundancy of data in a given grid cell. In this way, the integral bathymetric features are best accounted for. In the opposite situation, when there are less datapoints than gridpoints in a given area, we apply a triangulation interpolation method. The triangulation network is designed in such a way, that minimum triangle side lengths are achieved. Thus, maximum correlation between the numerical bathymetry and known bathymetric datapoints is then obtained.

We apply a graphical interactive program that allows a user to select a sequence of data files and to control the interpolation areas and the interpolation method. Resulting bathymetries on the curvilinear grid are shown by way of isolines. Depth values of individual samples or gridpoints can be corrected interactively.

Generation of boundary conditions

There are four basic types of boundary conditions, each of which is to be applied in different situations, in different combinations. These conditions are:

- water level "boundaries"
- velocity "boundaries"
- flux "boundaries"
- Riemann boundaries (weakly reflective boundaries).

The choice of the type of boundary condition depends on the phenomena to be studied. Mostly, one wants to prescribe the type of boundary condition that gives best driving force of the phenomena to be modelled. For instance, when modelling water levels at the inland side of an estuary, one prescribes the known water levels at the entrance of the estuary. However, the same internal solution may be achieved by prescribing flow velocities or fluxes or weakly reflective boundaries. The latter three yield a much weaker type of control over the final solution to be reached, however, since velocities are only weakly coupled to water levels, especially for the more complex flow situations.

Other examples are:
When modelling riverflow, one prescribes fluxes in combination with water levels.
When modelling crossflow in front of a harbour, one prescribes velocities.

If there is more than one open boundary for a certain problem, one often should not apply the same type of boundary condition at all boundaries. For instance, two velocity boundaries at both ends of a straight channel may lead to continuity problems if the fluxes, that are a result of these velocities and their respective water levels, are not compatible. Then it is better to prescribe velocities at one end of the channel and water levels at the other. A stable result is obtained. When modelling tidal flow in a large basin, forcing by prescribing only water levels is generally sound.

In practice, the type of boundary condition just depends of the availability of data. For instance, most of the larger sea models can only be driven by water level boundaries since these are the only quantities known at the sea boundaries. An example is the Total Irish Sea Model, that is driven on both the northern and southern boundaries by water levels.

When prescribing water level boundaries only, one should keep in mind that in nature and in the model alike, water level is a globally varying variable and behaves rather stiffly, i.e. there is a large correlation between water levels in locations that are not far apart. This means that a small error in the prescription of water levels can only be compensated by (large) responses of the internal forces in the model. This may lead to high velocities in order to compensate for the introduced pressure gradients at the boundaries. The area of influence of this phenomenon is not related to a certain number of gridsizes, but to the physical area of influence of a certain error in water level.

We apply a graphical interactive program that allows a user to select a sequence of data file and to control the interpolation areas and the interpolation method. Resulting bathymetrie on the curvilinear grid are shown by way of isolines. Depth values of individual sample or gridpoints can be corrected interactively.

Generation of boundary conditions

There are four basic types of boundary conditions, each of which is to be applied different situations, in different combinations. These conditions are:

- water level "boundaries"
- velocity "boundaries"
- flux "boundaries"
- Riemann boundaries (weakly reflective boundaries).

The choice of the type of boundary condition depends on the phenomena to be studie Mostly, one wants to prescribe the type of boundary condition that gives best driving for of the phenomena to be modelled. For instance, when modelling water levels at the inla side of an estuary, one prescribes the known water levels at the entrance of the estua However, the same internal solution may be achieved by prescribing flow velocities or flu or weakly reflective boundaries. The latter three yield a much weaker type of control o the final solution to be reached, however, since velocities are only weakly coupled to wa levels, especially for the more complex flow situations.

Other examples are:
When modelling riverflow, one prescribes fluxes in combination with water levels.
When modelling crossflow in front of a harbour, one prescribes velocities.

If there is more than one open boundary for a certain problem, one often should not ap the same type of boundary condition at all boundaries. For instance, two velocity bounda at both ends of a straight channel may lead to continuity problems if the fluxes, that ar result of these velocities and their respective water levels, are not compatible. Then i better to prescribe velocities at one end of the channel and water levels at the other. A st result is obtained. When modelling tidal flow in a large basin, forcing by prescribing c water levels is generally sound.

In practice, the type of boundary condition just depends of the availability of data. instance, most of the larger sea models can only be driven by water level boundaries s these are the only quantities known at the sea boundaries. An example is the Total Irish Model, that is driven on both the northern and southern boundaries by water levels.

When prescribing water level boundaries only, one should keep in mind that in nature in the model alike, water level is a globally varying variable and behaves rather stiffly, there is a large correlation between water levels in locations that are not far apart. means that a small error in the prescription of water levels can only be compensate (large) responses of the internal forces in the model. This may lead to high velocities in o to compensate for the introduced pressure gradients at the boundaries. The area of influ of this phenomenon is not related to a certain number of gridsizes, but to the physical of influence of a certain error in water level.

Introduction of check-stations, special hydraulic constructions etc.

The set-up of a hydrodynamic model is completed when all hydrodynamic features like dams, breakwaters, hydraulic jumps, outfalls etc. are introduced into the model. Furthermore, the positions of check stations or control sections, at which time-series of measurements are available have to be specified. In the calibration/verification model results are checked against these field data.

Use of collected field data

The hydrodynamic TRISULA model set-up as outlined in the above sections, needs to be calibrated and verified before it can be used in investigations and studies. In this process the simulated results are often compared to measurements of water levels and velocities. Discrepancies are minimized by tuning primarily the boundary conditions and local and global bathymetry. Secondly the Chezy parameter (bottom friction), viscosity and diffusivity coefficients are adjusted.

3.2 Assumptions and restrictions

The solution of the discretized equations of motion is only an approximation to the exact solution. The accuracy of the solution depends not only on the numerical scheme used, but also on the way in which the bottom topography, the geographical area and the physical processes are modelled.

The numerical scheme that is applied is of the ADI type. This means that water levels and velocities in the x-direction are implicitly solved in the first half time step, while water levels and velocities in the y-direction are solved in the second half time step.
This computational procedure strongly influences the wave propagation when applying a large time step. The assumption is made that, by restricting the computional time step, the wave can be propagated correctly, see (Stelling et al., 1986).

The open boundaries in a hydrodynamic model are fictitious in the sense that they are introduced to limit the water area that is modelled, and that in nature the flow passes through these boundaries completely unhindered. In the model, wave reflections may occur at these boundaries, which causes negative effects on the results. In TRISULA a user definable parameter is available which diminishes these effects. Furthermore, the number of tidal openings in an open boundary must be sufficiently large to prevent circulation of the current along the boundary.
Care must be taken when time-series of measurements are directly prescribed at the boundaries. Measurements often contain a lot of unwanted noise, due to meteorological or other effects. For tidal flow computations, calibration on processed field data obtained from a tidal analysis, avoids this problem.

The prescribed initial values and the boundary conditions at the start time of the simulation do not match the solution of the equations themselves. This will introduce a large spurious wave in the model: the spin effect. Subsequently the wave will be reflected at the internal boundaries and along the open boundaries of the model until the wave energy is dissipated completely by bottom or internal friction forces. These reflections can be observed as spurious oscillations in the solutions and they will determine the spin-up time of the model. To reduce this time, a smooth transition period can be specified by the user, during which the boundary conditions will be adapted gradually, starting from the prescribed initial condition value. This will somewhat reduce the spin-up time.

References

DELFT HYDRAULICS, 1992. TRISULA, A Simulation Program for Hydrodynamic Flows and Transports in 2 and 3 Dimensions. User Guide, Release 2.0. Delft, June 1992.

Eckart, C., 1958. Properties of water, Part II. The equation of state of water and sea water at low temperatures and pressures. American Journal of Science, 256:225-240, 1958.

Forestrer C.K., 1979. Higher Order Monotonic Convective Difference Schemes. Journal of Computational Physics, Vol. 23, 1979, 1-22.

Kolmogorov, A.N., 1942. Equations of turbulent motion in incompressible fluid, Izv. Akad. Nauk. SSR, Seria fizicheska Vi., No.1-2, pp 56-58 (English translation: 1968 Imperial College, Mech. Eng. Dept. Rept. ON/6).

Miles, J., 1987. Richardson's number revisited, In: Proc. 3rd Int. Symp. Stratified Flows, February 3-5, 1987, Pasedena, California.

Munk, W.H. and E.R. Anderson, 1948. Notes on the theory of the thermocline, J.of Marine Research, Vol.1.

Richardson, L.F., 1920. The supply of energy from and to atmospheric eddies, Proc. R. Soc. Lond., A97, pp 345-373.

Simonin, O., R.E. Uittenbogaard, F. Baron and P.L. Viollet, 1989 "Possibilities and limitations to simulate turbulence fluxes of mass and momentum, measured in a steady stratified mixing layer", In Proc. XXIII IAHR Congress, Ottawa, August 21-25, published by National Research Council Cananda, pp A55-A62.

Stelling, G.S., 1984. On the construction of computational method for shallow water flow problems. Rijkswaterstaat communications, No. 35, The Hague, Rijkswaterstaat.

Stelling, G.S. and J.J. Leendertse, 1991. Approximation of Convective Processes by Cyclic ACI methods, Proceeding ASCE, Conference, Tampa.

Stelling, G.S., A.K. Wiersma, and J.B.T.M. Willemse, 1986. Practical aspects of accurate tidal computations. J. Hydr. Eng. Div., ASCE.

Taylor, G.I., 1931. Effect of variation in density on the stability of superposed streams of fluid, Proc. Camb. Phil. Soc., 23, pp 730-731; Scientific Papers 2, pp 219-239.

Uittenbogaard, R.E., J.A.TH.M. van Kester, and G.S. Stelling, 1992. Implementation of three turbulence models in 3D-TRISULA for rectangular grids, report Z81/Z162, DELFT HYDRAULICS, May 1992.